

# The Anti-de Sitter Gott Universe: A Rotating BTZ Wormhole

**Sören Holst**

Fysikum, Stockholms Universitet  
Vanadisvägen 9, Box 6730, S-11385 Stockholm

E-mail: holst@physto.se

and

**Hans-Jürgen Matschull**

Institut für Physik, Johannes Gutenberg-Universität  
Staudingerweg 7, D-55099 Mainz

E-mail: matschul@thep.physik.uni-mainz.de

## Abstract

Recently it has been shown that a 2+1 dimensional black hole can be created by a collapse of two colliding massless particles in otherwise empty anti-de Sitter space. Here we generalize this construction to the case of a non-zero impact parameter. The resulting spacetime, which may be regarded as a Gott universe in anti-de Sitter background, contains closed timelike curves. By treating these as singular we are able to interpret our solution as a rotating black hole, hence providing a link between the Gott universe and the BTZ black hole. When analyzing the spacetime we see how the full causal structure of the interior can be almost completely inferred just from considerations of the conformal boundary.

## Outline

The Gott universe [1] and the BTZ black hole [2, 3] are two well known solutions to Einstein's equations in 2+1 dimensions, the latter involving a cosmological constant. Both can be constructed by identifying points in some originally maximally symmetric spacetime. Thus, starting from three dimensional Minkowski space, cutting out two wedges in an appropriate way and identifying their faces, yields the Gott universe. It can be regarded as a spacetime containing two point particles passing each other at a finite distance. What makes this spacetime remarkable is that when the particles' energy is sufficiently large, then it contains closed timelike curves. Hence, it is often referred to as the Gott time machine.

The BTZ solution on the other hand is constructed from anti-de Sitter space. It may be thought of as the negatively curved analogue to the Misner universe [4], or Grant space [5]. It is obtained from anti-de Sitter space by taking the quotient with respect to a discrete isometry group generated by a single element. The resulting spacetime is interesting since, contrary to its flat space cousins, it may be interpreted as a black hole. This is due to the exotic structure of the anti-de Sitter infinity. In the sense of conformal compactifications, spacelike and lightlike infinity of anti-de Sitter space coincide. They form the surface of the cylinder, which has its own causal structure. This is very different from the situation in Minkowski space. However, in order for the black hole interpretation to go through, one must agree to regard the subset of the spacetime that is filled with closed timelike curves, which result from taking the quotient, as singular.

In this paper we want to present a solution that reveals the close relation between these two spacetimes, the Gott time machine and the BTZ black hole. Essentially, what we are going to do is to perform the Gott construction in anti-de Sitter space instead of Minkowski space. In order to simplify the discussion we will take our particles to be massless, moving on lightlike geodesics. We then treat the resulting spacetime from the BTZ point of view. That is, instead of considering it to be a time machine, we declare the subset containing the closed timelike curves to be singular. This enables us to interpret our solution as a black hole with horizons. Since it is locally isometric to anti-de Sitter space, its exterior region will be that of a BTZ black hole.

From this point of view, our solution also furnishes the rotating generalization of the black hole formed by colliding point particles [6]. Together with earlier results [7], this implies that the three dimensional BTZ black holes not only share many important properties with ordinary, four dimensional black holes. They can also be formed by a matter collapse. The advantage of the three dimensional toy model with point particles is that the collapse can be described as an exact solutions to Einstein's equation, with the matter being reduced to a very simple, and in fact minimal system, just consisting of two massless point particles. This could finally allow a fully dynamical description, in which the physical degrees of freedom of the particles are treated as variables, and of which the spacetime we are going to construct is just a special, though generic, solution.

Let us give a brief summary of the construction of our spacetime, called  $\mathcal{S}$ . The main ideas

can also be read off from in the figures. In section 1, we begin by introducing a certain set of coordinates on anti-de Sitter space, called  $\mathcal{S}_0$ . They allow a very simple description of light rays, and turn out to be very useful for the construction of  $\mathcal{S}$ . In these coordinates, anti-de Sitter space is represented as the interior of a timelike cylinder whose constant time slices are Klein discs. The boundary of this cylinder, called  $\mathcal{J}_0$ , represents lightlike and spacelike infinity, and is also referred to as the conformal boundary of  $\mathcal{S}_0$ . We investigate lightlike geodesics and find that a null plane in  $\mathcal{S}_0$  can be defined by the family of all light rays that emerge from a point on  $\mathcal{J}_0$  (figure 1).

We also study the group structure of anti-de Sitter space, which is quite useful for the description of geodesics, isometries, and Killing vectors. In particular we are interested in lightlike isometries, the analogue to null rotations in Minkowski space, and put some effort in understanding their action on  $\mathcal{J}_0$  (figure 2). With this preparation, we perform the very construction of the spacetime  $\mathcal{S}$  in section 2. It contains two massless particles traveling in opposite directions on lightlike geodesics. Since such geodesics traverse the whole space, from one side of the cylinder to the other, in a finite coordinate time, the particles appear from infinity at some time, pass each other at a non-zero distance, and disappear again at a later time. In this sense, all the interesting physics takes place within a finite coordinate time interval.

The gravitational field of a point particle in three dimensional gravity, with or without cosmological constant, can be constructed by cutting out a wedge from a maximally symmetric spacetime and identifying its faces [8, 9]. In the case of a massless particle, we use a wedge that is degenerate to a null half plane [10], which is uniquely determined by the lightlike worldline of the particle. We cut anti-de Sitter space along such a surface, and then we identify the points on its lower face with those on its upper face according to the action of a null rotation. The result is that an observer who passes through this cut surface is effectively mapped backwards in time. To perform this construction for two particles, we can easily arrange the cut surfaces in such a way that they do not overlap (figure 3).

In section 3, we concentrate on the causal structure of the spacetime  $\mathcal{S}$ . A convenient way to do this is first to analyze the causal structure of its conformal boundary  $\mathcal{J}$ . Since the cut surfaces intersect with the boundary of the cylinder, and since an observer crossing one of them is effectively mapped backward in time, one easily sees how a lightlike or timelike curve winding around the boundary may close. It is not difficult to locate the region to which all closed timelike curves on  $\mathcal{J}$  are confined (figure 4). We then discuss how this information can be used in order to find the causal structure of the interior of  $\mathcal{S}$ . We find that there is a chronology horizon in  $\mathcal{S}$ , behind which every point lies on a closed timelike curve. The horizon can be constructed in a remarkably simple way. We just have to evolve null planes from appropriate points at  $\mathcal{J}$  (figures 5 and 6). This is very different from the situation in the flat Gott universe, where the location of the CTC region are quite cumbersome [11].

Finally, in section 4, we change our point of view, and interpret the region containing the closed timelike curves as a singularity. It turns out to be a naked singularity inside a timelike wormhole, which connects two otherwise separate regions of spacetime. The particles them-

selves are passing from one region to the other, through the wormhole. The interior of the wormhole is separated from one exterior region by a black hole event horizon, and from the second exterior region by a white hole event horizon (figure 7). The event horizon emerges from a cusp, which is located on the spacelike geodesic that connects the particles in the moment when they fall into the black hole, respectively when they fall out of the white hole (figure 8). The properties of the wormhole, such as its horizon length and angular velocity, can be computed as functions of the energy and the minimal distance, or impact parameter, of the particles. To complete the discussion, we shall also consider an extremal (figure 9), and a static black hole (figure 10).

## 1 Anti-de Sitter Space

To introduce the notation, let us give a brief description of three dimensional anti-de Sitter space, denoted by  $\mathcal{S}_0$ . It can be covered by a global, cylindrical coordinate chart  $(t, \chi, \varphi)$ , with  $\chi \geq 0$  and  $\varphi \equiv \varphi + 2\pi$ . It has a constant negative curvature, and the metric with signature  $(-, +, +)$  is

$$ds^2 = d\chi^2 + \sinh^2\chi d\varphi^2 - \cosh^2\chi dt^2. \quad (1.1)$$

A somewhat different coordinate system, which is more appropriate for the description of light rays, is obtained by replacing the hyperbolic radial coordinate  $0 \leq \chi < \infty$  by an angle  $0 \leq \theta < \pi/2$ . The relation between  $\chi$  and  $\theta$  can be written in as

$$\tan \theta = \sinh \chi, \quad \sin \theta = \tanh \chi, \quad \cos \theta \cosh \chi = 1, \quad (1.2)$$

which are all equivalent. Inserting this into (1.1) gives

$$ds^2 = \frac{d\theta^2 + \sin^2\theta d\varphi^2 - dt^2}{\cos^2\theta} \quad (1.3)$$

This tells us that anti-de Sitter space is conformally isometric to the direct product of a real time axis and a Euclidean half sphere of radius one. With the sphere embedded in  $\mathbb{R}^3$ , we can say that the conformal factor is the inverse square of the  $z$ -coordinate. The conformally transformed metric reads

$$d\tilde{s}^2 = d\theta^2 + \sin^2\theta d\varphi^2 - dt^2. \quad (1.4)$$

Including the equator as a boundary, we obtain a conformal compactification of  $\mathcal{S}_0$ . Its boundary is called  $\mathcal{J}_0$ . It represents spatial infinity as well as the origin and destination of light rays.

### Light rays

As lightlike geodesics are not affected by conformal transformations, we can say that the *optical geometry* of anti-de Sitter space is that of a Euclidean half sphere [12]. Every light ray travels

along a grand circle with a constant velocity of one. The fact that the boundary  $\mathcal{J}_0$  is also a grand circle implies that every light ray on  $\mathcal{S}_0$  intersects  $\mathcal{J}_0$  at two antipodal points, and the time that it takes to travel from one side to the other is  $\pi$ . Moreover, all light rays emerging from a point on  $\mathcal{J}_0$  at some time  $t$  meet again at the antipodal point at  $t + \pi$ . We call this a *family* of light rays.

With a slight modification, the spherical coordinate system can be adapted to a special class of such families. Instead of representing the slices of constant  $t$  by the northern hemisphere, we take it to be the eastern hemisphere. The latitude then runs from the north to the south pole, such that  $0 < \theta < \pi$ , and for the longitude we have  $0 < \varphi < \pi$ . The metric (1.3) is almost unchanged. Only the conformal factor in front, which was formerly given by the inverse square of the  $z$ -coordinate, now becomes the inverse square of the  $y$ -coordinate. In terms of the rotated coordinates we have

$$ds^2 = \frac{d\theta^2 + \sin^2\theta d\varphi^2 - dt^2}{\sin^2\theta \sin^2\varphi}. \quad (1.5)$$

The conformally transformed metric (1.4) is unchanged. What is quite useful to know is that the original hyperbolic coordinate  $\chi$  is now related to the spherical coordinates by

$$\cosh \chi = \frac{1}{\sin \theta \sin \varphi}. \quad (1.6)$$

The new coordinates are regular all over  $\mathcal{S}_0$ , as can be seen in figure 1(a). The coordinate singularities at the poles  $N$  and  $S$  are on the boundary. The lines of constant longitude  $\varphi$  are now the paths of light rays connecting the poles, and the lines of constant latitude  $\theta$  at time  $t$  are the wave fronts of the families of light rays that started off from the north pole at  $t - \theta$ , and will arrive at the south pole at  $t - \theta + \pi$ .

The disc below is obtained from the half sphere by orthogonal projection. It is the so called *Klein disc*, which is very closely related to the *Poincaré disc* [13]. The latter has already been used in previous work [6, 14, 15]. It can be obtained by stereographic instead of orthogonal projection. The special properties of the Klein disc, to which we shall stick within this article, are not of particular importance. The only special feature that is useful, but not necessary to know is that spatial geodesics are represented as straight lines on the disc. This is the case, for example, for the wave fronts belonging to a family of light rays, which are the lines of constant latitude  $\theta$ . The main purpose we use the Klein disc for is to draw three dimensional pictures of anti-de Sitter space.

We represent  $\mathcal{S}_0$  as a product of a Klein disc with a real line, which becomes an infinitely long cylinder, whose boundary is  $\mathcal{J}_0$ . The time interval between  $t = 0$  and  $t = \pi$  is shown in figure 1(b). The surface  $s$  inside the cylinder is spanned by a family of light rays. They emerge from the north pole at  $t = 0$ , denoted by  $X$ , and arrive at the south pole at  $t = \pi$ , called  $Y$ . The surface is defined by the simple coordinate equation  $\theta = t$ . The vertical lines on  $s$  are the lines of constant  $\varphi$ , representing the individual light rays. The horizontal lines are those of constant  $t$

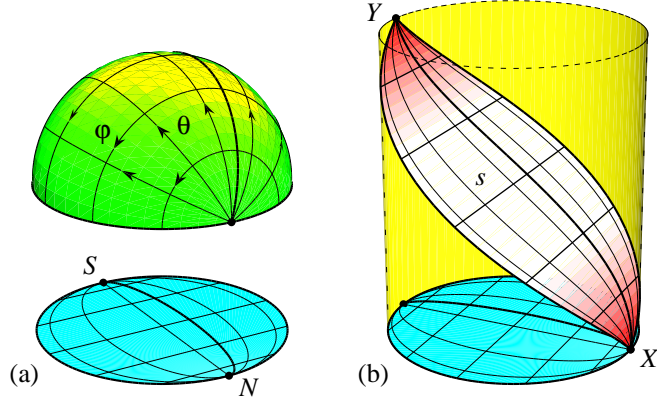


Figure 1: The spherical coordinates  $(t, \theta, \varphi)$  on the half sphere, the Klein disc, and the null plane  $s$  spanned by the family of light rays connecting the antipodal points  $X$  and  $Y$  on  $\mathcal{J}_0$ . The bold line is the path of a light ray.

and  $\theta$ , representing the wave fronts at different times. The induced metric on the surface can be expressed in terms of the coordinates  $t$  and  $\varphi$ . With  $\theta = t$  in (1.5), we find that

$$ds = d\varphi / \sin \varphi. \quad (1.7)$$

It is of rank one because the surface is lightlike. The fact that it only depends on  $\varphi$  implies that the light rays belonging to a family are *parallel*. Like in Minkowski space, a surface spanned by a family of parallel light rays in anti-de Sitter space is called a *null plane*. It can be regarded as the future or past light cone attached to a point on the boundary  $\mathcal{J}_0$ . We call  $X$  the *origin* and  $Y$  the *destination* of the null plane  $s$ . The part of anti-de Sitter space above  $s$  is the future of  $X$ , and the part below  $s$  is the past of  $Y$ . What is quite remarkable is that this also defines a causal structure on  $\mathcal{J}_0$  itself.

The lines where the null plane intersects with the boundary of the cylinder can be considered as two special light rays belonging to the family, with  $\varphi = 0$  and  $\varphi = \pi$ . They travel counter clockwise, respectively clockwise with a velocity of one along  $\mathcal{J}_0$ . We can also see this when we look at the conformally transformed metric on the boundary. For both  $\varphi = 0$  and  $\varphi = \pi$ , the metric (1.4) becomes  $d\tilde{s}^2 = d\theta^2 - dt^2$ . This implies that there are right and left moving light rays on  $\mathcal{J}_0$ , with  $|d\theta/dt| = 1$ . This is a feature of anti-de Sitter space that has no counterpart in Minkowski space, where spacelike and lightlike infinity are not the same, and lightlike infinity splits into two disconnected components, one representing the origin and the other the destination of light rays. Neither of them has an internal causal structure.

## The group structure

A very different way to think about anti-de Sitter space is as a group manifold. It is isometric to the matrix group  $\mathrm{SL}(2)$  of real  $2 \times 2$  matrices with unit determinant. In terms of the spherical coordinates, the isometry  $\mathcal{S}_0 \rightarrow \mathrm{SL}(2)$  is explicitly given by

$$\mathbf{x}(t, \theta, \varphi) = \frac{\cos t \mathbf{1} + \sin t \gamma_0 + \cos \theta \gamma_1 + \sin \theta \cos \varphi \gamma_2}{\sin \theta \sin \varphi}, \quad (1.8)$$

where  $\mathbf{1}$  is the unit matrix, and the gamma matrices form an orthonormal basis of the associated Lie algebra  $\mathfrak{sl}(2)$  of traceless matrices,

$$\gamma_0 = \begin{pmatrix} 0 & 1 \\ -1 & 0 \end{pmatrix}, \quad \gamma_1 = \begin{pmatrix} 0 & 1 \\ 1 & 0 \end{pmatrix}, \quad \gamma_2 = \begin{pmatrix} 1 & 0 \\ 0 & -1 \end{pmatrix}. \quad (1.9)$$

One can check by straightforward calculation that the metric (1.5) is equal to the induced Cartan Killing metric

$$ds^2 = \frac{1}{2} \mathrm{Tr}(\mathbf{x}^{-1} d\mathbf{x} \mathbf{x}^{-1} d\mathbf{x}), \quad (1.10)$$

and therefore the map  $\mathcal{S}_0 \rightarrow \mathrm{SL}(2)$  is an isometry. However, the two manifolds are only locally isometric. It is obvious from (1.8) that the coordinate  $t$  becomes periodic on  $\mathrm{SL}(2)$ . To obtain  $\mathcal{S}_0$  from  $\mathrm{SL}(2)$ , one has to unwind its fundamental loop. Hence, anti-de Sitter space is the covering manifold of the group  $\mathrm{SL}(2)$ . In practice, we do not have to care about this very much, because all our constructions will take place within a time interval of  $\pi$ , and therefore the period of  $2\pi$  in  $t$  cannot be seen.

The probably most useful feature of the group structure is that it allows a very simple description of isometries and Killing vectors. A generic time and space orientation preserving isometry of  $\mathrm{SL}(2)$  can be written as

$$f : \mathbf{x} \mapsto \mathbf{u}^{-1} \mathbf{x} \mathbf{v}, \quad (1.11)$$

where  $\mathbf{u}$  and  $\mathbf{v}$  are two arbitrary group elements. If  $\mathbf{u} = e^{\mathbf{m}}$  and  $\mathbf{v} = e^{\mathbf{n}}$  are exponentials of some elements  $\mathbf{m}, \mathbf{n} \in \mathfrak{sl}(2)$ , then the action of  $f$  can be written as the flow of a Killing vector field  $\xi$ . This can be defined by

$$\xi(\mathbf{x}) = \mathbf{x} \mathbf{n} - \mathbf{m} \mathbf{x}, \quad (1.12)$$

where  $\mathbf{x}$  is considered as an  $\mathrm{SL}(2)$  valued function on  $\mathcal{S}_0$ . Note that this determines  $\xi$  uniquely, and implies that for the flow of  $\xi$ , denoted by  $e^{\tau \xi}$ ,  $\tau \in \mathbb{R}$ , we have

$$e^{\tau \xi}(\mathbf{x}) = e^{-\tau \mathbf{m}} \mathbf{x} e^{\tau \mathbf{n}}. \quad (1.13)$$

For  $\tau = 1$ , this is equal to (1.11). Given a second isometry  $g : \mathbf{x} \mapsto \mathbf{g}^{-1} \mathbf{x} \mathbf{h}$ ,  $\mathbf{g}, \mathbf{h} \in \mathrm{SL}(2)$ , we can compute its action on the vector field  $\xi$ . For the push forward  $g^*(\xi)$ , we must have

$$e^{\tau g^*(\xi)} = g \circ e^{\tau \xi} \circ g^{-1}, \quad (1.14)$$

which implies that

$$g^*(\xi)(x) = x(h^{-1}n h) - (g^{-1}m g)x. \quad (1.15)$$

Hence, the two vectors  $m, n \in \mathfrak{sl}(2)$  transform independently under the adjoint representation of  $g, h \in \mathrm{SL}(2)$ . If we interpret them as vectors in three dimensional Minkowski space, which is isometric to  $\mathfrak{sl}(2)$ , then the transformations

$$g^* : \quad m \mapsto g^{-1}m g, \quad n \mapsto h^{-1}n h, \quad (1.16)$$

can be considered as proper Lorentz transformations in  $\mathfrak{sl}(2)$ . They preserve the invariant lengths  $\frac{1}{2}\mathrm{Tr}(m^2)$  and  $\frac{1}{2}\mathrm{Tr}(n^2)$  of  $m$  and  $n$ . Given two Killing vectors  $\xi_1$  and  $\xi_2$ , we can also compute their scalar product using the formula (1.10),

$$\begin{aligned} \xi_1 \cdot \xi_2 &= \frac{1}{2} \mathrm{Tr}(x^{-1} \xi_1(x) x^{-1} \xi_2(x)) \\ &= \frac{1}{2} \mathrm{Tr}(n_1 n_2 + m_1 m_2 - x^{-1} m_1 x n_2 - x^{-1} m_2 x n_1). \end{aligned} \quad (1.17)$$

This is a scalar function on  $\mathcal{S}_0$ . Its limit on the boundary  $\mathcal{J}_0$  will in general diverge, because of the zero denominator in (1.8). However, under a certain condition, namely

$$\alpha m_1 = \beta m_2, \quad \alpha n_1 = -\beta n_2, \quad \alpha, \beta \in \mathbb{R}, \quad (1.18)$$

the scalar product is constant, equal to the sum of the scalar products of the Minkowski vectors  $m$  and  $n$ , and it remains finite at the boundary. We then call the two Killing vectors *asymptotically orthogonal*, or orthogonal on  $\mathcal{J}_0$ . In fact, if we first derive the limits of  $\xi_1$  and  $\xi_2$  on  $\mathcal{J}_0$ , and then take their scalar product with respect to the conformally transformed metric (1.4), then they turn out to be orthogonal.

## Geodesics

Another useful property of isometries, or Killing vectors on the group manifold is that their fixed points, if there are any, always form a geodesic. We call this the *axis* of the isometry. Vice versa, every geodesic is the axis of some isometry. This is again similar to Minkowski space, where every straight line is the axis of a one parameter family of Poincaré transformations. To see that this is also the case in anti-de Sitter space, consider the fixed point equation for the isometry  $f$  defined above, respectively its generating Killing vector  $\xi$  in the form

$$u x = x v \quad \Leftrightarrow \quad m x = x n. \quad (1.19)$$

It can be solved if and only if  $u$  and  $v$  lie in the same conjugacy class of  $\mathrm{SL}(2)$ , or equivalently if the vectors  $m$  and  $n$  in  $\mathfrak{sl}(2)$  are related by a proper Lorentz transformation. Let us assume this, and that it is not one of the trivial classes  $u = v = \pm 1$ , or  $m = n = 0$ . Otherwise there are either no fixed points at all, or  $f = \mathrm{id}$  and  $\xi = 0$ . To show that the solutions to (1.19) form a



geodesic, we pick a particular solution  $\mathbf{y}$  and replace the variable  $\mathbf{x}$  by  $\mathbf{z} = \mathbf{x}\mathbf{y}^{-1}$ . The relation between  $\mathbf{x}$  and  $\mathbf{z}$  is again an isometry. It is therefore sufficient to show that the solutions for  $\mathbf{z}$  lie on a geodesic. The equation for  $\mathbf{z}$  can then be written as

$$\mathbf{u}\mathbf{z} = \mathbf{z}\mathbf{u} \quad \Leftrightarrow \quad \mathbf{m}\mathbf{z} = \mathbf{z}\mathbf{m}, \quad (1.20)$$

where we have used that  $\mathbf{u}\mathbf{y} = \mathbf{y}\mathbf{v}$ , or equivalently  $\mathbf{m}\mathbf{y} = \mathbf{y}\mathbf{n}$ . Hence,  $\mathbf{z}$  is required to commute with  $\mathbf{m}$ , or its exponential  $\mathbf{u}$ . In a Lie group of rank one, this is the case for all  $\mathbf{z}$  belonging to the unique one-dimensional subgroup that contains  $\mathbf{u}$ , which is that generated by the exponential of the element  $\mathbf{m}$  of the algebra. On the other hand, a one dimensional subgroup of a Lie group is a geodesic passing through the unit element. This proves that the fixed points form a geodesic.

To see that every geodesic is the axis of some isometry, take some geodesic and choose two distinct points  $\mathbf{y}$  and  $\mathbf{z}$  thereon, such that  $\mathbf{u} = \mathbf{z}\mathbf{y}^{-1}$  and  $\mathbf{v} = \mathbf{y}^{-1}\mathbf{z}$  are different from  $\pm\mathbf{1}$ . The fixed point equation (1.19) is then solved by  $\mathbf{y}$  and  $\mathbf{z}$ , which means that the axis of this isometry is the unique geodesic passing through  $\mathbf{y}$  and  $\mathbf{z}$ . There is a one parameter family of such isometries, as can be seen by varying  $\mathbf{z}$  and  $\mathbf{y}$  along the geodesic. A priori, this provides two parameters, but one can easily convince oneself that a variation of  $\mathbf{y}$  can always be compensated by a variation of  $\mathbf{z}$  and vice versa, so that actually there is only one parameter. As in Minkowski space, this can be regarded as the *angle of rotation*.

### Null isometries

Whether the axis of an isometry is a timelike, lightlike, or spacelike geodesic depends on the conjugacy class to which  $\mathbf{u}$  and  $\mathbf{v}$  belong. The lightlike ones are of particular interest for us. As an example, consider the following two positive lightlike group elements,

$$\mathbf{u} = \mathbf{1} + e^{-\delta} \tan \epsilon (\gamma_0 - \gamma_2), \quad \mathbf{v} = \mathbf{1} + e^{\delta} \tan \epsilon (\gamma_0 + \gamma_2), \quad (1.21)$$

where  $\delta$  and  $0 < \epsilon < \pi/2$  are two real parameters. Both  $\mathbf{u}$  and  $\mathbf{v}$  lie on the future light cone of the unit element  $\mathbf{1} \in \text{SL}(2)$ , belonging to the same conjugacy class. The reason for choosing the parameters in this particular way will become clear later on. We expect that the axis of the corresponding *null isometry* is a lightlike geodesic. Using the representation of  $\mathbf{x}$  in terms of the spherical coordinates (1.8), the fixed point equation becomes

$$\mathbf{u}\mathbf{x} = \mathbf{x}\mathbf{v} \quad \Leftrightarrow \quad \cos \theta = \cos t, \quad \sin \theta \cos \varphi = \sin t \tanh \delta. \quad (1.22)$$

The first equation can always be solved for  $\theta$ , which ranges from 0 to  $\pi$ . It tells us that the geodesic is oscillating with a period of  $2\pi$  between the north and the south pole. As these points do not belong to  $\mathcal{S}_0$ , the curve actually splits into a series of geodesics, each within a time interval of  $\pi$ . For  $0 < t < \pi$ , the coordinate equations can then be simplified to

$$\mathbf{u}\mathbf{x} = \mathbf{x}\mathbf{v} \quad \Leftrightarrow \quad \theta = t, \quad \cos \varphi = \tanh \delta. \quad (1.23)$$

Obviously, this is one of the light rays belonging to the family considered above. The first equation defines the null plane  $s$  in figure 1(b), and the second equation picks out a particular light ray. The parameter  $\delta$  increases from  $-\infty$  in the front of the picture to  $+\infty$  in the back. In the limits  $\delta \rightarrow \pm\infty$ , we also recover the two light rays traveling along  $\mathcal{J}_0$ . What is useful to know is that  $\delta$  measures the physical distance between the individual light rays. To see this, we have to express the metric (1.7) on the null plane in terms of  $\delta$  instead of  $\varphi$ ,

$$ds = d\varphi/\sin\varphi = -d\cos\varphi/\sin^2\varphi = -\cosh^2\delta d\tanh\delta = -d\delta. \quad (1.24)$$

The minus sign appears because  $\varphi$  decreases with increasing  $\delta$ . Coming back to the isometry specified by  $\delta$  and  $\epsilon$ , we can say that the parameter  $\delta$  determines the location of the axis of  $f$ , and we expect  $\epsilon$  to specify the angle of rotation.

In Minkowski space, the action of a lightlike rotation on the unique null plane that contains the axis is such that each light ray in that plane is a fixed line. The points on the null plane are shifted along the light rays by an amount that is proportional to the angle of rotation and the distance from the axis. To see that this is also the case in anti-de Sitter space, let us make the following ansatz. On the surface  $s$ , we introduce the coordinates  $t$  and  $\varphi$ , such that a point with spherical coordinates  $(t, t, \varphi)$  is simply denoted by  $(t, \varphi)$ . It is then represented by the group element

$$\mathbf{x}(t, \varphi) = \frac{\cot t (\mathbf{1} + \gamma_1) + \gamma_0 + \cos\varphi \gamma_2}{\sin\varphi}, \quad (1.25)$$

which is obtained from (1.8) with  $\theta = t$ . Now, assume that  $f$  maps a point  $\mathbf{x}_- = \mathbf{x}(t_-, \varphi)$  onto  $\mathbf{x}_+ = \mathbf{x}(t_+, \varphi)$  on the same light ray. This yields the following relation between the time coordinates,

$$\mathbf{x}_- \mathbf{v} = \mathbf{u} \mathbf{x}_+ \quad \Leftrightarrow \quad \cot t_+ - \cot t_- = 2 \tan\epsilon (\cosh\delta \cos\varphi - \sinh\delta). \quad (1.26)$$

For  $0 < t < \pi$ , this provides a one-to-one relation between  $t_-$  and  $t_+$ . From this we conclude that the ansatz was correct. The null plane  $s$  is indeed a fixed surface of  $f$ , and the individual light rays belonging to the family are fixed lines. The points are shifted along the light rays by an amount that increases with the angle of rotation and the distance from the axis. Note that on the axis we have  $\cos\varphi = \tanh\delta$ , and therefore  $t_+ = t_-$ . Apart from the fact that the amount of shift is not proportional to the parameters, the situation is the same as in Minkowski space.

We can also ask the reverse question. Given a light ray, what is the most general isometry, or Killing vector, that has this light ray as a fixed line? Or, more generally, what is the most general isometry that has a fixed light ray? This will be useful to know at several points in the derivation of the physical properties of our wormhole spacetime. The first observation we can make is that whenever there is a fixed light ray of some isometry  $f$ , then all members of its family are fixed lines of  $f$  as well. The argument is the same as above. The null plane containing the given light ray is a fixed surface of  $f$ , because there is only one such null plane, and the physical distances

between the members of the family are preserved. So, the actual question is, which isometries have a family of fixed light rays?

Let us give an explicit answer for the special family of light rays spanning the null plane  $s$  defined above, and then generalize the result. As an ansatz, consider the action of a Killing vector  $\xi$  defined by (1.12). To see whether  $\xi$  is tangent to the given family of light rays, we have to evaluate  $\xi(x)$  on  $s$ , express this as a function of the coordinates  $(t, \varphi)$  on  $s$ , as defined by (1.25), and check whether the result is proportional to  $d\mathbf{x}/dt$ . It turns out that this is the case if and only if the Minkowski vectors  $\mathbf{m}$  and  $\mathbf{n}$  defining the Killing vector  $\xi$  are of the form

$$\mathbf{m} = a(\gamma_0 - \gamma_2) + c\gamma_1, \quad \mathbf{n} = b(\gamma_0 + \gamma_2) - c\gamma_1, \quad (1.27)$$

with real numbers  $a, b, c$ . Explicitly, the action of the Killing vector  $\xi$  on the light rays in  $s$  is then given by

$$d \cot t = (a + b) \cos \varphi + (a - b) - 2c \cot t. \quad (1.28)$$

With  $a = e^{-\delta} \tan \epsilon$ ,  $b = e^{\delta} \tan \epsilon$ , and  $c = 0$ , we can easily integrate this and recover the action (1.26) of  $f = e^{\xi}$ . We then also have  $\mathbf{u} = e^{\mathbf{m}}$  and  $\mathbf{v} = e^{\mathbf{n}}$ , with  $\mathbf{u}$  and  $\mathbf{v}$  given in (1.21).

To generalize this result, we have to find the properties which are common to all Minkowski vectors (1.27), and which are invariant under isometries of anti-de Sitter space. We know that under a general isometry  $g : \mathbf{x} \mapsto \mathbf{g}^{-1}\mathbf{x}\mathbf{h}$ , the vectors  $\mathbf{m}$  and  $\mathbf{n}$  transform under proper Lorentz rotations (1.16). The only invariants under such transformations are the length of  $\mathbf{m}$  and  $\mathbf{n}$ , and in the case of lightlike and timelike vectors we have to distinguish between positive and negative ones. Now, it turns out that the vectors given above are always lightlike or spacelike and of the same length,

$$\text{Tr}(\mathbf{m}^2) = \text{Tr}(\mathbf{n}^2) \geq 0. \quad (1.29)$$

Moreover, if they are lightlike, then we can have any combination of positive and negative lightlike vectors. Hence, we expect that (1.29) is a necessary and sufficient condition for a Killing vector to have a family of fixed light rays. Indeed, given a Killing vector  $\xi$  with  $\mathbf{m}$  and  $\mathbf{n}$  fulfilling (1.29), then we can always find an isometry  $g : \mathbf{x} \mapsto \mathbf{g}^{-1}\mathbf{x}\mathbf{h}$  such that  $\mathbf{g}^{-1}\mathbf{m}\mathbf{g}$  and  $\mathbf{h}^{-1}\mathbf{n}\mathbf{h}$  are of the form (1.27), for some parameters  $a, b, c$ . The Killing vector  $g^*(\xi)$  is then tangent to the light rays in  $s$ , which implies that  $\xi$  has a family of fixed light rays, namely those spanning the null plane  $g^{-1}(s)$ .

### Isometries acting on $\mathcal{J}_0$

Finally, let us also give a brief description of the action of a null isometry on the conformal boundary  $\mathcal{J}_0$  of  $\mathcal{S}_0$ . If we cut the boundary of the cylinder in figure 1 along a vertical line and lay it down on a plane, we get an infinitely long strip. Again for  $0 < t < \pi$ , this is shown in figure 2. To recover the cylinder surface, the left and right margins must be identified, so that everything that leaves the strip to the right reappears on the left and vice versa. A disadvantage of our spherical coordinate system is that it does not provide proper coordinates on  $\mathcal{J}_0$ , because

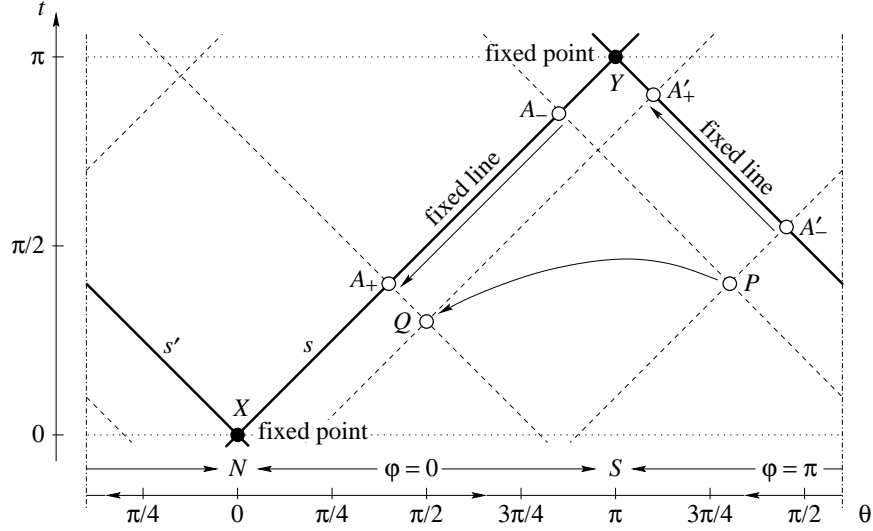


Figure 2: The action of a null isometry on  $\mathcal{J}_0$ . The fixed lines  $s$  and  $s'$  are the intersections of the null plane in figure 1 with the boundary of the cylinder. The fixed points  $X$  and  $Y$  are the end points of the axis. The image  $Q = f(P)$  of a point  $P$  on  $\mathcal{J}_0$  can be constructed when the action of  $f$  on the fixed light rays is known.

the poles are located there. However, for most of the constructions to be made on  $\mathcal{J}_0$ , it is sufficient to use the time coordinate  $t$ .

The bold lines denoted by  $s$  and  $s'$  in figure 2 are the intersections of the null plane in figure 1(b) with the boundary of the cylinder. They represent a left and a right moving light ray on  $\mathcal{J}_0$ . We already know that these are fixed lines of  $f$ . If  $A_-$  and  $A_+$  are two points on  $s$  such that  $A_+ = f(A_-)$ , then their time coordinates satisfy

$$\cot t_+ - \cot t_- = 2e^{-\delta} \tan \epsilon. \quad (1.30)$$

This follows from (1.26) with  $\varphi = 0$ . Similarly, if  $A'_-$  and  $A'_+$  are two points on  $s'$ , such that  $A'_+ = f(A'_-)$ , then the relation between their time coordinates is

$$\cot t'_+ - \cot t'_- = -2e^{\delta} \tan \epsilon, \quad (1.31)$$

which is obtained from (1.26) with  $\varphi = \pi$ . It is useful to keep in mind what the directions of these transformations are. For positive  $\epsilon$ , points on  $s$  are shifted *downwards*, and those on  $s'$  are shifted *upwards*.

The intersections  $X$  and  $Y$  of the two light rays are the fixed points of  $f$ . This is where the axis of  $f$  intersects with  $\mathcal{J}_0$ . Quite generally, a fixed point of an isometry on  $\mathcal{J}_0$  is always at the

intersection of a left and a right moving fixed light ray, and vice versa the two light rays passing through a fixed point are fixed lines. If we extend the light rays  $s$  and  $s'$ , we find that  $f$  has more fixed points. There are two intersections within each time period of  $2\pi$ . However, as already mentioned, all the interesting physics will take place within the time interval  $0 < t < \pi$ , and therefore it is sufficient to consider this region only.

Knowing the action of  $f$  on the fixed light rays  $s$  and  $s'$ , we can easily construct the image  $Q = f(P)$  of any point  $P$  on  $\mathcal{J}_0$ . The fixed light rays divide  $\mathcal{J}_0$  into a series of *diamonds*. The continuity of  $f$  implies that  $P$  and  $Q$  lie in the same diamond. Now, consider the two light rays passing through  $P$  and denote their intersection with the fixed lines by  $A_-$  and  $A'_-$ , as indicated in figure 2. The images of these light rays are those that pass through  $A_+ = f(A_-)$  and  $A'_+ = f(A'_-)$ , determined by (1.30) and (1.31). It follows that the image of  $P$  is at the only intersection  $Q$  of the light rays through  $A_+$  and  $A'_+$  within the same diamond.

## 2 The Spacetime

We are now ready to construct our spacetime manifold  $\mathcal{S}$ . What we are looking for is a solution to Einstein's equations with a negative cosmological constant and two massless, pointlike particles as matter sources. In three dimensions, such a spacetime has a constant negative curvature everywhere, except for two conical singularities located on the world lines of the particles. It can be constructed from anti-de Sitter space  $\mathcal{S}_0$  by *cutting* and *gluing* [8, 16]. For each particle, one has to choose a world line and a so called *wedge*. The wedge is a region of  $\mathcal{S}_0$  which is bounded by two *faces*, that is, two surfaces extending from the world line to infinity, such that one of them is mapped onto the other by an isometry, whose axis is the world line.

Taking away the interior of the wedges and identifying the points on the faces according to the corresponding isometries, one obtains a spacetime  $\mathcal{S}$  which is locally isometric to  $\mathcal{S}_0$ , but with conical singularities located on the world lines. This method has already been used to describe the collapse of two colliding particles into a static black hole [6]. Here, we want to generalize it to the case of two non-colliding particles approaching each other and collapsing into a rotating black hole. It turns out that in this case the black hole is actually a timelike wormhole with a naked singularity therein. The particles pass through the wormhole into a second exterior region. To begin with, let us give a definition of the spacetime  $\mathcal{S}$ .

### Massless particles

There are two physically relevant parameters describing the relative motion of two massless point particles passing each other. Namely, their distance at the moment of closest approach and their centre of mass energy. The distance is the length of the unique spacelike geodesic that is orthogonal to both lightlike world lines. For two identical particles, the centre of mass frame can be defined as follows. It is that coordinate system  $(t, \theta, \varphi)$  in which the particles are

interchanged by reflection at the time axis, or rotation of the cylinder by 180 degrees,

$$r : (t, \theta, \varphi) \mapsto (t, \pi - \theta, \pi - \varphi), \quad \mathbf{x} \mapsto \gamma_0^{-1} \mathbf{x} \gamma_0. \quad (2.1)$$

Note that the reflection is an involution,  $r \circ r = \text{id}$ , but not a parity transformation. Within the centre of mass frame, we still have the freedom to perform time shifts and spatial rotations. Using this, we can achieve that the spacelike geodesic joining the particles at the moment of closest approach is the coordinate line  $t = \theta = \pi/2$ . This is the horizontal line in the centre of the null plane in figure 1(b). One of the world lines is then a member of the family spanning this surface, and the second one is obtained by reflection. Both can be specified as the axes of appropriate isometries,

$$f_1 : \mathbf{x} \mapsto \mathbf{u}_1^{-1} \mathbf{x} \mathbf{v}_1, \quad f_2 : \mathbf{x} \mapsto \mathbf{u}_2^{-1} \mathbf{x} \mathbf{v}_2. \quad (2.2)$$

The parameters for the first particle are those already introduced in (1.21),

$$\mathbf{u}_1 = \mathbf{1} + e^{-\delta} \tan \epsilon (\gamma_0 - \gamma_2), \quad \mathbf{v}_1 = \mathbf{1} + e^{\delta} \tan \epsilon (\gamma_0 + \gamma_2). \quad (2.3)$$

The second isometry is determined by  $r \circ f_2 = f_1 \circ r$ , which implies that

$$\mathbf{u}_2 = \mathbf{1} + e^{-\delta} \tan \epsilon (\gamma_0 + \gamma_2), \quad \mathbf{v}_2 = \mathbf{1} + e^{\delta} \tan \epsilon (\gamma_0 - \gamma_2). \quad (2.4)$$

The coordinate equations for the world lines are

$$p_1 : \theta = t, \quad \cos \varphi = \tanh \delta, \quad p_2 : \theta = \pi - t, \quad \cos \varphi = -\tanh \delta. \quad (2.5)$$

From the results of the previous section, it follows that the physical distance between the particles at the moment of closest approach is  $2\delta$ . The second parameter  $\epsilon$  measures the centre of mass energy of the particles. It specifies the angle of rotation of  $f_1$  and  $f_2$ , and therefore the *size* of the wedges to be cut out. It is not so important what the precise definition of the centre of mass energy in a curved spacetime is, and what the relations are between  $\epsilon$ , the momenta of the particles and the properties of the conical singularities [6, 8, 9]. It is sufficient to know that, at least qualitatively,  $\epsilon$  measures the amount of energy contained in the combined system.

### The cut surfaces

For massless particles moving on lightlike world lines, the wedges can be chosen in a special way. Let us from now on assume that  $\delta > 0$ , and consider the following *null half planes*,

$$s_1 : \theta = t, \quad \cos \varphi \geq \tanh \delta, \quad s_2 : \theta = \pi - t, \quad \cos \varphi \leq -\tanh \delta. \quad (2.6)$$

These are two non-overlapping lightlike surfaces extending from the world lines to  $\mathcal{J}_0$ , as shown in figure 3. We already know that the half plane  $s_1$  is a fixed surface of  $f_1$ , and due to the

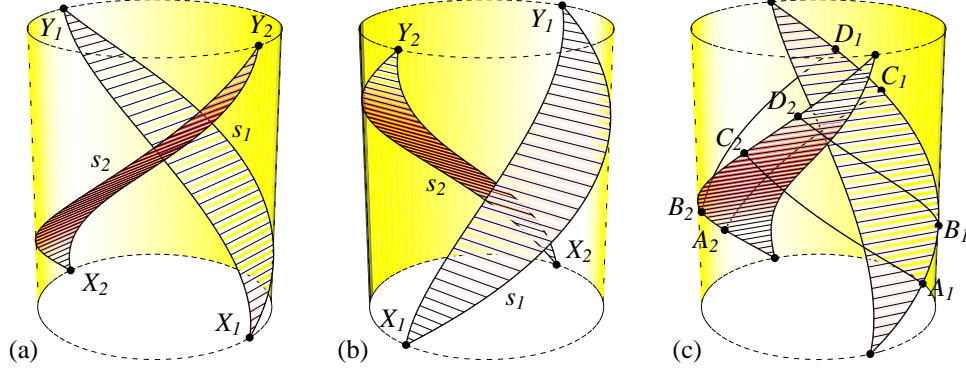


Figure 3: The spacetime  $\mathcal{S}$  is constructed from  $\mathcal{S}_0$  by cutting and gluing along the null half planes  $s_1$  and  $s_2$  (a,b). They extend from the world lines  $p_1$  and  $p_2$  to the boundary. The solid lines (c) on the boundary are the two closed light rays constructed in figure 4. Here and in all following figures, the lines drawn on surfaces are lines of constant time coordinate  $t$ .

symmetry under reflection  $s_2$  is a fixed surface of  $f_2$ . On both surfaces, we introduce coordinates  $t$  and  $\varphi$ , such that a point  $(t, t, \varphi) \in s_1$  is denoted by  $(t, \varphi)$ , and the rotated point  $(t, \pi - t, \pi - \varphi) \in s_2$  is also denoted by  $(t, \varphi)$ . When written in these coordinates, the action of  $f_2$  on  $s_2$  is formally the same as that of  $f_1$  on  $s_1$ , namely

$$f_{1,2}: (t_-, \varphi) \mapsto (t_+, \varphi), \quad \cot t_+ - \cot t_- = 2 \tan \epsilon (\cosh \delta \cos \varphi - \sinh \delta). \quad (2.7)$$

To construct the spacetime  $\mathcal{S}$ , we consider the half planes  $s_1$  and  $s_2$  as two *degenerate* wedges. There is then no interior of the wedges to be removed. Instead, the points on the upper and the lower faces of the null planes are considered as distinct. The identification of the faces is such that a point  $(t_-, \varphi)$  on the *lower* face corresponds to the point  $(t_+, \varphi)$  on the *upper* face of the same null half plane. Note that for a lightlike surface there is a well defined distinction between the upper and lower face, the former being the one that points towards the future, and the latter being that pointing towards the past.

The resulting spacetime  $\mathcal{S}$  is still covered by a single spherical coordinate chart  $(t, \theta, \varphi)$ , but now in a non-trivial way. The coordinates are discontinuous along the cut surfaces. They can be considered as self-overlap regions, with the transition functions given by (2.7). As a result,  $\mathcal{S}$  contains two conical singularities located on lightlike world lines of massless particles. Their centre of mass energy is  $\epsilon$ , and they pass each other at a distance of  $2\delta$ . Perhaps we should also mention that the degenerate wedges are very similar to the gravitational shock waves carried by massless particles in higher dimensions [17, 18]. The gravitational field of such a particle can also be constructed by cutting and gluing.

The cut surface is thereby also the unique null hyperplane that contains the world line. However, the map that provides the identification is not an isometry of the underlying symmetric space, which is either Minkowski or anti-de Sitter space. As a consequence, additional curvature in form of a gravitational shock wave is introduced on the cut surface. This is not the case in three dimensions. Here, it is possible to choose the coordinates such that the cut surface becomes a *half* plane, attached to one side of the world line only. This is quite essential, because otherwise the two cut surfaces would overlap, and the cutting and gluing procedure would not work for two particles simultaneously. It is also a nice way to see that there is no interaction between the particles by local forces.

### 3 The Gott Universe

Regarding the construction of the spacetime manifold, we are now already finished. This is probably a bit surprising. It is not at all obvious that there are any of the typical features of a wormhole, such as a singularity, horizons, or a kind of tunnel connecting otherwise separate regions of spacetime. Moreover, it seems that there cannot be any singularity at all, except for the harmless ones on the world lines, because the spacetime is constantly curved. In fact, we have to introduce the wormhole singularity in a somewhat artificial way, which is however quite standard in the construction of three dimensional black holes. Before doing so, let us have a closer look at our spacetime manifold  $\mathcal{S}$  as it is, from a slightly different point of view.

What we have constructed is the anti-de Sitter analogue of the *Gott universe* [1, 19]. The Gott universe is a spacetime with two point particles and vanishing cosmological constant. It can be constructed from Minkowski space by essentially the same cutting and gluing procedure. Provided that the centre of mass energy of the particles exceeds a certain threshold, it contains closed timelike curves. They fill a region that extends from spatial infinity to some neighbourhood of the particles at the moment of closest approach. That there is a certain danger for this to happen in our spacetime as well can be inferred from the relation (2.7). The essential point is that the points on the lower faces with time coordinate  $t_-$  are mapped onto points on the upper faces with a *smaller* time coordinate  $t_+$ .

As a consequence, a future pointing timelike curve, approaching one of the cut surfaces from below, continues above the cut surface at an earlier time. We can say that when passing over the cut surfaces, we *gain* time. Doing so several times, it might be possible to form a closed timelike curve. This is indeed what is going to happen, provided that the energy of the particles is large enough, and, in contrast to the Gott universe where this is already sufficient, the distance between the particles has to be small. In other words, a sufficiently large amount of energy has to be located in a small volume. This is a typical condition for a black hole to be created. The purpose of this section is to find the exact condition to be imposed on the energy and the distance, and to determine the subset of  $\mathcal{S}$  which is filled by the closed timelike curves.



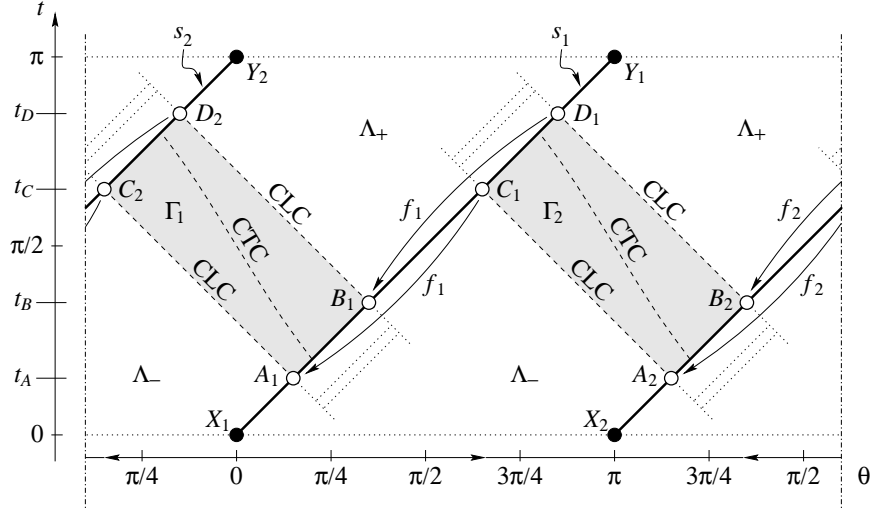


Figure 4: The boundary  $\mathcal{J}$  of  $\mathcal{S}$  is obtained from the boundary  $\mathcal{J}_0$  of  $\mathcal{S}_0$  by cutting and gluing along the right moving light rays  $s_1$  and  $s_2$ . The left moving light rays  $A_1C_2A_2C_1$  and  $B_1D_2B_2D_1$  are closed lightlike curves on  $\mathcal{J}$ . The shaded region  $\Gamma = \Gamma_1 \cup \Gamma_2$  is filled with closed timelike curves.

### The causal structure of $\mathcal{J}$

A convenient way to find the condition for closed timelike curves to arise is to look at the conformal boundary  $\mathcal{J}$  of  $\mathcal{S}$ . This can be constructed from the boundary  $\mathcal{J}_0$  of  $\mathcal{S}_0$  by the following cutting and gluing procedure. Figure 4 represents the boundary of the cylinder in figure 3. The bold lines are the intersections of the cut surfaces  $s_1$  and  $s_2$  with the boundary. They extend from the points  $X_{1,2}$  at  $t = 0$ , where the particles emerge, to the points  $Y_{1,2}$  at  $t = \pi$ , where they disappear again. Along these lines the boundary is cut. The identification is such that a point with time coordinate  $t_-$  below one of the cuts is identified with a point with time coordinate  $t_+$  above the cut. According to (1.30), the relation between  $t_-$  and  $t_+$  is

$$\cot t_+ - \cot t_- = 2e^{-\delta} \tan \epsilon. \quad (3.1)$$

When the cut is traversed from below, this is always a shift backward in time,  $t_+ < t_-$ . The crucial question is whether a left moving light ray on  $\mathcal{J}$  can gain enough time by passing over the cuts to form a loop. The time that it takes for such a light ray to travel from one cut to the other is always  $\pi/2$ . This must be equal to the time gained when passing over the cut,  $t_- - t_+ = \pi/2$ . Inserting this into (3.1), we find that

$$\sin(2t_+) = -\sin(2t_-) = e^\delta \cot \epsilon. \quad (3.2)$$

There is no solution if the right hand side is bigger than one. The time gained is then always smaller than  $\pi/2$ , and therefore it is not possible for a light ray to form a closed loop. In particular, this is the case for small energies or large distances, which is quite reasonable. In fact, in both limits  $\epsilon \rightarrow 0$  and  $\delta \rightarrow \infty$ , the particles disappear and  $\mathcal{S}$  becomes equal to empty anti-de Sitter space  $\mathcal{S}_0$ .

For closed light rays on  $\mathcal{J}$  to exist, the energy must be bigger than  $\pi/4$ , so that  $\tan \epsilon > 1$ . This is also the threshold for a static black hole to be formed by colliding particles [6]. Here we get the additional condition that the spatial separation of the particles must be sufficiently small,  $e^\delta < \tan \epsilon$ . Then we have the situation shown in figure 4. There are two closed light rays  $A_1C_2A_2C_1$  and  $B_1D_2B_2D_1$ , where

$$A_1 = f_1(C_1), \quad B_1 = f_1(D_1), \quad A_2 = f_2(C_2), \quad B_2 = f_2(D_2), \quad (3.3)$$

and for the time coordinates we have

$$t_C = t_A + \pi/2, \quad t_D = t_B + \pi/2. \quad (3.4)$$

To determine the location of these points explicitly, it is useful to replace the parameters  $\delta$  and  $\epsilon$  by two positive real numbers  $0 < \mu < \nu$ , such that

$$\cosh(\mu/2) = e^{-\delta} \tan \epsilon, \quad \cosh(\nu/2) = e^\delta \tan \epsilon. \quad (3.5)$$

Note that the right hand sides of both equations are bigger or equal to one if  $\delta \geq 0$  and  $e^\delta \leq \tan \epsilon$ . We can then solve the equations (3.2) and (3.4), and find that

$$\cot t_A = e^{\mu/2}, \quad \cot t_B = e^{-\mu/2}, \quad \cot t_C = -e^{-\mu/2}, \quad \cot t_D = -e^{\mu/2}. \quad (3.6)$$

An alternative and rather elegant way to characterize the light rays that form the closed loops on  $\mathcal{J}$  is the following. When considered as light rays on  $\mathcal{J}_0$ , that is, before the cutting and gluing procedure is carried out, they are fixed lines of certain combinations of the isometries  $f_1$ ,  $f_2$  and the reflection  $r$ . Let us define

$$g_1 = f_1 \circ r = r \circ f_2, \quad g_2 = f_2 \circ r = r \circ f_1. \quad (3.7)$$

If we now act with  $r$  on the relations (3.3), and use that for all points  $P$  with indices 1 and 2 we have  $r(P_1) = P_2$  and  $r(P_2) = P_1$ , then we find that

$$A_1 = g_1(C_2), \quad B_1 = g_1(D_2), \quad A_2 = g_2(C_1), \quad B_2 = g_2(D_1). \quad (3.8)$$

It follows that the left moving light rays  $A_1C_2$  and  $B_1D_2$ , extended beyond these points, are fixed lines of  $g_1$ . Similarly, the extended light rays  $A_2C_1$  and  $B_2D_1$  are fixed lines of  $g_2$ . In other words, the light rays which, after the cutting and gluing procedure, form the closed

light rays on  $\mathcal{J}$  are those left moving light rays on  $\mathcal{J}_0$ , which are fixed lines of the combined isometries  $g_1$  and  $g_2$ .

The conformal boundary  $\mathcal{J}$  of  $\mathcal{S}$  splits into three open subsets  $\Lambda_-$ ,  $\Gamma$ , and  $\Lambda_+$ , separated by the two closed light rays, as indicated in figure 4. In the shaded region  $\Gamma = \Gamma_1 \cup \Gamma_2$ , the time gained when passing over the cuts is even bigger than  $\pi/2$ . This has two consequences. First of all, there are also closed timelike curves in that region. One such curve is shown in the figure. Moreover, consider a left moving light ray in  $\Gamma$ . After each winding, it appears a little bit earlier, so that effectively it travels backwards in time. Asymptotically, it approaches the lower closed light ray. A timelike curve can have the same behaviour. It follows that the causal structure of  $\Gamma$  is completely degenerate. Every two points in  $\Gamma$  can be connected by a future pointing timelike curve.

### Closed timelike curves

The fact that there are closed timelike curves on  $\mathcal{J}$  implies that such curves also exist in  $\mathcal{S}$ . Consider, for example, the closed timelike curve shown in figure 4, and shift it, by a continuous deformation, away from the boundary into the interior of the cylinder. For a sufficiently small deformation parameter it will still be timelike, and thus it becomes a closed timelike curve in  $\mathcal{S}$ . The natural question that arises is which part of  $\mathcal{S}$  is filled with closed timelike curves. The boundary of that region is called the *chronology horizon*. As we shall see, and also according to some general theorems [11, 20], the chronology horizon is a lightlike surface that consists of pieces of null planes.

To see where it is located, let us first summarize some properties of closed timelike curves. A quite general feature is that, within a *connected* region filled with closed timelike curves, the causal structure is always completely degenerate. We saw this already in the case of the region  $\Gamma$  on  $\mathcal{J}$ . In general, let  $\Delta$  be a connected subset of some spacetime, such that through each point  $P \in \Delta$  there passes a closed timelike curve. For each point  $P \in \Delta$ , we define the subset  $\Delta_P \subset \Delta$  containing all points  $Q \in \Delta$  such that there is a closed timelike curve passing through  $P$  and  $Q$ . It follows immediately from the definition that  $P \in \Delta_P$ , and given two points  $P$  and  $Q$ , then  $\Delta_P$  and  $\Delta_Q$  are either equal or disjoint.

Moreover,  $\Delta_P$  is always an open subset of  $\Delta$ . If a point  $Q$  is connected to  $P$  along a closed timelike curve, then this is also true for some neighbourhood of  $Q$ . For example, take the intersection of the future light cone of some point on the curve shortly before  $Q$  with the past light cone of some other point shortly after  $Q$ . This is a non-empty open set containing  $Q$  and contained in  $\Delta_P$ . From all this it follows that  $\Delta = \bigcup_{P \in \Delta} \Delta_P$  is a decomposition of  $\Delta$  into non-empty, disjoint, open subsets. As  $\Delta$  is assumed to be connected, this is only possible if  $\Delta_P = \Delta$  for all  $P \in \Delta$ . Hence, every two points in  $\Delta$  are connected along a closed timelike curve. Or, equivalently, for every two points  $P, Q \in \Delta$  there is a future pointing timelike curve from  $P$  to  $Q$ .

What does this imply for the chronology horizon in our spacetime manifold? In the appendix

we show that the subset  $\Delta \subset \mathcal{S}$ , which is defined to be the union of all closed timelike curves, is indeed connected. It then follows that  $\Delta$  is exactly that region of  $\mathcal{S}$  which is *causally connected* to  $\Gamma \subset \mathcal{J}$ . By causally connected we mean the set of all points  $P \in \mathcal{S}$  such that a signal can be sent from  $\Gamma$  to  $P$  and from  $P$  to  $\Gamma$ . As  $\Gamma$  is an open subset of  $\mathcal{J}$ , it is thereby sufficient to consider signals traveling on timelike curves. The proof splits into two parts. First we have to show that, given a point  $P \in \mathcal{S}$  which is causally connected to  $\Gamma$ , then there is a closed timelike curve passing through  $P$ . And secondly, we have to show that every point on a closed timelike curve in  $\mathcal{S}$  is causally connected to  $\Gamma$ .

The first part is quite easy. By assumption, there is a future pointing timelike curve from some point  $O \in \Gamma$  to  $P$  and from there to another point  $Q \in \Gamma$ . On the other hand, we know that every two points on  $\Gamma$  are connected by a future pointing timelike curve in  $\Gamma$ . Hence, there exists a closed timelike curve through the points  $OPQ$ . Parts of this curve lie on  $\mathcal{J}$ . Using the same argument as above, we can deform it such that it becomes a closed timelike curve in  $\mathcal{S}$ , still passing through  $P$ . Hence, there is indeed a closed timelike curve in  $\mathcal{S}$  passing through every point which is causally connected to  $\Gamma$ . The reversed statement follows from the previously discussed general feature of closed timelike curves, applied to the subset  $\Delta \cup \Gamma$  of the compactified cylinder  $\mathcal{S} \cup \mathcal{J}$ . Since this is a connected region filled with closed timelike curves, it follows that every point  $P \in \Delta$  is causally connected to  $\Gamma$ .

Finally, a more special feature of closed timelike curves in  $\mathcal{S}$  gives us some qualitative information about the shape of  $\Delta$ . Every closed timelike curve in  $\mathcal{S}$  passes alternatingly over the two cut surfaces, and it never hits the world lines of the particles. The first property follows from the fact that there is no timelike curve in anti-de Sitter space which intersects a null plane twice. Hence, there cannot be any closed timelike curve in  $\mathcal{S}$  passing over the same cut surface twice without passing over the other in between. Moreover, if a closed timelike curve intersects with a world line, then, by the same argument, it cannot pass over the cut surface attached to *this* world line before or after the intersection. But then it has to pass twice over the *other* cut surface without a time jump in between, which is also impossible. All together, it is therefore reasonable to expect that  $\Delta$  is some torus like region surrounding the particles. This is also what it looks like in the flat Gott universe.

### The covering of $\Gamma$

Let us now explicitly find the future and the past of  $\Gamma$ . Consider a point  $P \in \mathcal{S}$ , for example in the neighbourhood of the rectangle  $\Gamma_1$  in figure 4. That is,  $P$  lies in the *interior* of the cylinder, but close enough to the boundary so that it makes sense to say that  $P$  lies *above* the surface  $s_1$  and *below*  $s_2$ . We can then ask whether a signal can be sent from  $\Gamma$  to  $P$ . Or, in other words, whether  $\Gamma$  can be seen from  $P$ . If  $P$  lies in the future of the point  $A_1$  on the boundary, then this is certainly possible. Now assume that it is not possible to reach  $P$  from  $A_1$ . Then it might still be possible to reach it from some point in the rectangle  $\Gamma_2$ , by passing through the cut surface  $s_1$ . As seen from  $P$ , the rectangle  $\Gamma_2$  behind the cut surface  $s_1$  appears to be at the location

$$f_1(\Gamma_2) = f_1(r(\Gamma_1)) = g_1(\Gamma_1).$$

This is the first dotted rectangle beyond the points  $A_1$  and  $B_1$  in figure 4. For a signal to be sent from  $\Gamma_2$  through  $s_1$  to  $P$ , it is sufficient for  $P$  to lie in the future of the lower corner of *this* rectangle. We can obviously proceed this way. A signal from  $\Gamma$  to  $P$  can also be sent from  $\Gamma_1$ , by passing through the cut surface  $s_2$  and then through  $s_1$ . This is possible if  $P$  lies in the future of the lower corner of the rectangle  $f_1(f_2(\Gamma_1)) = g_1^2(\Gamma_1)$ . This is the apparent position of  $\Gamma_1$  as seen from  $P$ , by looking through  $s_1$  and then through  $s_2$ . Allowing the signal to wind around arbitrarily many times, we find that it is sufficient for the point  $P$  in the interior of the cylinder to lie in the future of the lower corner of at least one of the rectangles  $g_1^n(\Gamma_1)$  on the boundary, where  $n$  is a non-negative integer. It then also lies in the future of all such rectangles with larger  $n$ .

Vice versa, we can ask the question as to whether a signal can be sent from  $P$  to  $\Gamma$ . If the point  $P$  inside the cylinder lies in the past of  $D_2$  on the boundary, then the signal can be sent directly to  $\Gamma_1$ . If we allow the signal to pass once over  $s_2$ , it is sufficient for  $P$  to lie in the past of the upper corner of the rectangle  $f_2^{-1}(\Gamma_2) = g_1^{-1}(\Gamma_1)$ . This is the apparent position of  $\Gamma_2$  when looking from  $P$  through the cut surface  $s_2$ . To send a signal from  $P$  through  $s_2$  and  $s_1$  to  $\Gamma_1$ ,  $P$  has to lie in the past of the upper corner of  $f_2^{-1}(f_1^{-1}(\Gamma_2)) = g_1^{-2}(\Gamma_1)$ , and so on. For a signal to be sent from  $P$  to  $\Gamma$  along any possible path, the condition is that  $P$  has to lie in the past of the upper corner of at least one of the rectangles  $g_1^{-n}(\Gamma_1)$ , again for some non-negative integer  $n$ .

All together, we can say that the *apparent shape* of the strip  $\Gamma$  on the boundary, as seen by an observer located above  $s_1$  and below  $s_2$  in the interior of the cylinder, is represented by the union of all rectangles  $g_1^n(\Gamma_1)$ ,  $n \in \mathbb{Z}$ . Similarly, we can make the same construction for an observer in the neighbourhood of  $\Gamma_2$ . For her, the strip appears to look like the union of the rectangles  $g_2^n(\Gamma_2)$ . Let us denote this by

$$\tilde{\Gamma}_1 = \bigcup_{n \in \mathbb{Z}} g_1^n(\Gamma_1), \quad \tilde{\Gamma}_2 = \bigcup_{n \in \mathbb{Z}} g_2^n(\Gamma_2). \quad (3.9)$$

Both  $\tilde{\Gamma}_1$  and  $\tilde{\Gamma}_2$ , considered as subsets of  $\mathcal{J}_0$ , represent the *covering space* of the strip  $\Gamma$  on  $\mathcal{J}$ . In fact, the quotient spaces  $\tilde{\Gamma}_1/g_1^2$  and  $\tilde{\Gamma}_2/g_2^2$  are, by construction, isometric to  $\Gamma$ . What does this covering space look like? It is a strip bounded by the extended left moving light rays  $A_1C_2$  and  $B_1D_2$ , respectively  $A_2C_1$  and  $B_2D_1$ . As these are fixed lines of  $g_1$ , respectively  $g_2$ , all the rectangles share them as their upper right and lower left edges. Furthermore, the rectangles fit together and form a continuous strip, because the lower right edge of each rectangle coincides with the upper left edge of the next one.

The crucial question is whether the strips are infinitely long or not. This depends on whether the isometries  $g_1$  and  $g_2$  have fixed points on  $\mathcal{J}_0$  or not. If they do, then the corners of the rectangles  $g_1^n(\Gamma_1)$  and  $g_2^n(\Gamma_2)$  converge to the first fixed points of  $g_1$  and  $g_2$  beyond the cuts. The strips are then of finite size. The most convenient way to find out whether there are any fixed points is to look for fixed right moving light rays of  $g_1$  and  $g_2$ . The fixed points are then

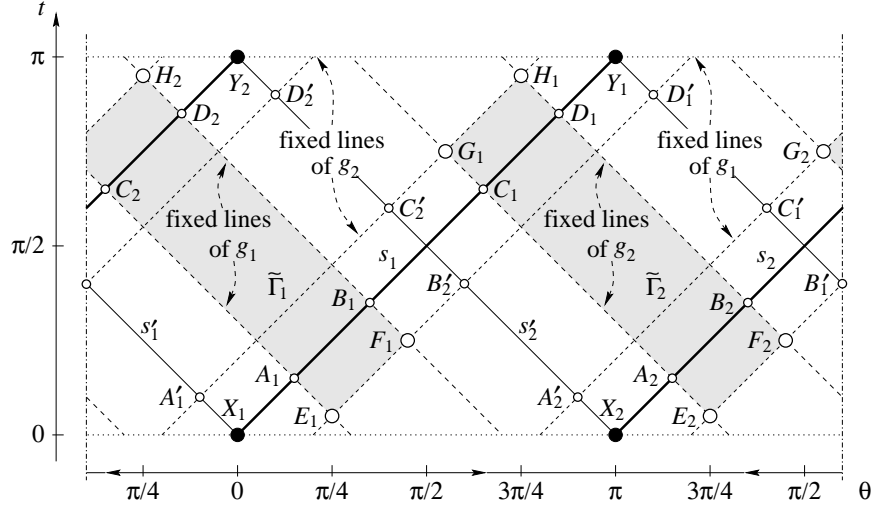


Figure 5: The construction of the fixed points  $E_1, F_1, G_2, H_2$  of  $g_1$ , and  $E_2, F_2, G_1, H_1$  of  $g_2$ . The solid lines are the fixed light rays of  $f_1$  and  $f_2$ , and the dashed lines are those of  $g_1$  and  $g_2$ . The shaded rectangles  $\tilde{\Gamma}_1$  and  $\tilde{\Gamma}_2$  represent the apparent shape of the region of closed timelike curves on  $\mathcal{J}$ , as seen by an observer in the interior of the cylinder, sitting in the neighbourhood of the rectangles  $\Gamma_1$  and  $\Gamma_2$  in figure 4.

at the intersections with the left moving ones, which we already know. Moreover, the first fixed right moving light rays beyond the cuts are then the upper left, respectively the lower right edges of the rectangles  $\tilde{\Gamma}_1$  and  $\tilde{\Gamma}_2$ .

To find the fixed right moving light rays, we repeat the construction of the left moving ones, with right and left interchanged. How did we find the left moving ones? We started from the cut lines  $s_1$  and  $s_2$  on  $\mathcal{J}_0$ . These are the *right* moving light rays connecting the points  $X$  and  $Y$ . They are once again shown as bold lines in figure 5. On these lines, we found the points  $A, B, C, D$ , determined by (3.6), such that  $f(C) = A, f(D) = B, t_C = t_A + \pi/2$  and  $t_D = t_B + \pi/2$ , with all indices equal to either 1 or 2. From this we concluded that the *left* moving light rays passing through  $A_1C_2$  and  $B_1D_2$  are fixed lines of  $g_1$ , and those passing through  $A_2C_1$  and  $B_2D_1$  are fixed lines of  $g_2$ .

Now, we repeat this construction starting from the *left* moving light rays  $s'_1$  and  $s'_2$  connecting the points  $X$  and  $Y$ . These are the thin solid lines in figure 5. We know already how the isometries  $f_1$  and  $f_2$  act on them. They are the opposite intersections of the null planes with the boundary of the cylinder. The action of  $f_1$  on  $s'_1$  and that of  $f_2$  on  $s'_2$  is given by (1.31). A point with time coordinate  $t'_-$  is mapped onto the one with time coordinate  $t'_+$ , where

$$\cot t'_+ - \cot t'_- = -2e^\delta \tan \epsilon. \quad (3.10)$$

In contrast to (3.1), this is a shift forward in time, and the amount of shift is larger. We can always find four points  $A'$ ,  $B'$ ,  $C'$ , and  $D'$  on each cut, such that

$$C'_1 = f_1(A'_1), \quad D'_1 = f_1(B'_1), \quad C'_2 = f_2(A'_2), \quad D'_2 = f_2(B'_2), \quad (3.11)$$

and with the time coordinates satisfying

$$t_{C'} = t_{A'} + \pi/2, \quad t_{D'} = t_{B'} + \pi/2. \quad (3.12)$$

The solution is similar to (3.6), we only have to replace  $\mu$  by the second parameter  $\nu$ , as defined in (3.5),

$$\cot t_{A'} = e^{\nu/2}, \quad \cot t_{B'} = e^{-\nu/2}, \quad \cot t_{C'} = -e^{-\nu/2}, \quad \cot t_{D'} = -e^{\nu/2}. \quad (3.13)$$

Note that  $\nu$  is related to  $\mu$  by interchanging  $\delta$  with  $-\delta$ . Up to an overall sign, this is also the relation between (3.10) and (3.1). The sign is taken care of by interchanging the points with their images. We have  $A = f(C)$  and  $B = f(D)$ , but  $C' = f(A')$  and  $D' = f(B')$ . As a consequence, the *right* moving light rays passing through  $A'_2C'_1$  and  $B'_2D'_1$  are now the fixed lines of  $g_1$ , and those passing through  $A'_1C'_2$  and  $B'_1D'_2$  are the fixed lines of  $g_2$ .

Finally, we find the relevant fixed points of  $g_1$  to be those denoted by  $E_1, F_1, G_2, H_2$  in figure 5. These are the limits to which the corners of the rectangles  $g_1^n(\Gamma_1)$  converge as  $n \rightarrow \pm\infty$ . The union  $\tilde{\Gamma}_1$  of all these rectangles is again a rectangle. Similarly,  $\tilde{\Gamma}_2$  is the rectangle with corners at  $E_2, F_2, G_1, H_1$ . These are the first fixed points of  $g_2$  beyond the cuts. For the time coordinates of the fixed points we have the relations

$$\begin{aligned} t_E = t_A - t_{A'} = t_C - t_{C'}, & \quad t_F = t_B - t_{A'} = t_D - t_{C'}, \\ t_G = t_C + t_{A'} = t_A + t_{C'}, & \quad t_H = t_D + t_{A'} = t_B + t_{C'}. \end{aligned} \quad (3.14)$$

Note that all these points lie in the time interval  $0 < t < \pi$ , which follows from (3.6) and (3.13), under the condition that  $\mu < \nu$ , which holds because of  $\delta > 0$ .

### The chronology horizon

It is now straightforward to find the region of  $\mathcal{S}$  that is causally connected to  $\Gamma$ , and thus the location of the chronology horizon. We have to evolve the past light cone  $c_+$  from the apparent position of the *last point* on  $\Gamma$ , respectively the future light cone  $c_-$  from the apparent position of the *first point* on  $\Gamma$ . Depending on which sides of the cut surfaces we are on, these are either the null planes emerging from  $E_1$  and arriving at  $H_2$ , or those emerging from  $E_2$  and arriving at  $H_1$ . The region that is enclosed by these null planes and the cut surfaces is the subset  $\Delta \subset \mathcal{S}$  that is filled by the closed timelike curves.

In figure 6(a), the shaded rectangles from figure 5, with the fixed points of the isometries  $g$  in the corners, are shown on the boundary of the cylinder. Evolving the null planes backwards

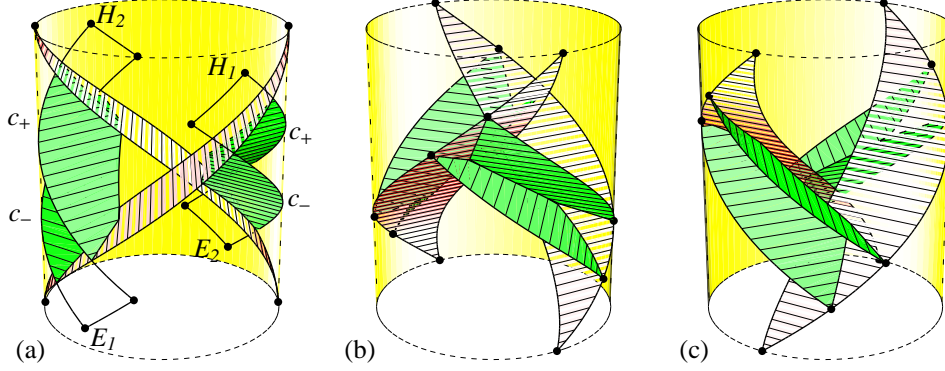


Figure 6: The chronology horizon consists of two null planes in  $\mathcal{S}$ , denoted by  $c_-$  and  $c_+$ . Each of them is defined piecewise, by gluing together appropriate parts of null planes in  $\mathcal{S}_0$  (a). For  $c_-$ , they originate from the points  $E_{1,2}$ , and for  $c_+$  their destinations are the points  $H_{1,2}$ . The horizon encloses the region  $\Delta$  of closed timelike curves, which has the shape of a triangular torus (b), that winds around the particles without touching them (c).

from  $H_1$  and  $H_2$ , and taking only the pieces that lie on the correct sides of the cut surfaces, we get the upper null plane  $c_+$  of the chronology horizon. What is important to note is that the two pieces fit together along the cut surfaces, forming a single null plane in  $\mathcal{S}$ . Consider, for example, the neighbourhood of the cut surface  $s_1$ . This is the one in the front of figure 6(a). Below  $s_1$ , the horizon is represented by a piece of the null plane with destination  $H_1$ . A piece of this plane immediately below  $s_1$  can be seen on the right side in figure 6(a).

It continues above  $s_1$ , as a piece of the null plane with destination  $H_2$ . This piece of the horizon  $c_+$  can be seen almost completely on the left side of figure 6(a). For these two pieces to form a single null plane in  $\mathcal{S}$ , without a kink at the intersection with the cut surface  $s_1$ , the lower part must be related to the upper part by the transition function  $f_1$ . This is in fact the case, because for the points  $H_1$  and  $H_2$  defining the null planes we have  $f_1(H_1) = g_1(r(H_1)) = g_1(H_2) = H_2$ . The last equation holds because, by definition,  $H_2$  is a fixed point of  $g_1$ . Similarly, one shows that  $c_+$  is smooth at the intersection with  $s_2$ , and thus a null plane in  $\mathcal{S}$ . The lower part  $c_-$  of the chronology horizon is defined in the same way.

Instead of the null planes with destinations  $H$ , we take appropriate pieces of those with origins  $E$ . They also form a single null plane in  $\mathcal{S}$ . It intersects with  $c_+$  along a special curve in  $\mathcal{S}$ . Being the intersection of two null planes, it is a spacelike geodesic. On the other hand, it is a closed loop. It is thus a spacelike closed geodesic, and in fact the only closed geodesic in  $\mathcal{S}$ . This is also where the horizon ends, because the points beyond that intersection are no longer causally connected to  $\Gamma$ . So, we can say that the chronology horizon extends from spatial



infinity to a closed spacelike geodesic that winds around the particles. Again, the chronology horizon of the flat Gott universe has exactly the same behaviour [11].

## 4 The BTZ Wormhole

Now we are going to change our point of view. Instead of considering the spacetime  $\mathcal{S}$  as a generalized Gott universe, we would like to think of it as a three dimensional black hole of the BTZ type. To do this, we have to interpret the region containing the closed timelike curves as a *singularity*. This is the typical procedure to construct three dimensional black holes. For example, to get a matter free black hole, one starts from empty anti-de Sitter space and divides it by the action of some discrete isometry group [2, 3, 15]. The quotient space typically contains closed timelike curves. To get a well defined causal structure, one takes away a subset through which all closed timelike curves have to pass, and interprets the boundary of that subset as a singularity.

We can do the same here. The question is then, which part of the region  $\Delta$  behind the chronology horizon do we have to take away in order to remove all closed timelike curves? In the case of the quotient space construction, with the isometries defined by one or several Killing vectors, one usually takes away the region where the Killing vectors are timelike. This region is obviously filled with closed timelike curves, namely the flow lines of the Killing vectors. On the other hand, one can show that every closed timelike curve must pass through this region. However, even in the simplest case of only one Killing vector, the singular subset to be removed is not *minimal*, in the sense that there is no smaller set through which all closed timelike curves pass.

In fact, such a minimal subset does not exist, and therefore the only motivation to choose the one defined by the timelike Killing vectors is to preserve the symmetries of the spacetime. If we want make a similar construction here, we first have to deal with the problem that our spacetime is not the quotient space of anti-de Sitter space with respect to some discrete isometry group. However, a part of it turns out to have a rotational symmetry. There exists a unique rotational Killing field  $\xi_{\text{rot}}$ , with the property that  $e^{2\pi\xi_{\text{rot}}} = \text{id}$ . In other words, at least a part of our spacetime looks exactly like a part of a rotating vacuum BTZ wormhole, which is obtained as a quotient space of anti-de Sitter space with respect to the isometry generated by  $\xi_{\text{rot}}$ .

Of course, this Killing field cannot be defined globally on  $\mathcal{S}$ , because obviously our spacetime does not possess a continuous rotational symmetry. But it can be defined within a sufficiently large subset, which includes the region of closed timelike curves. An explicit construction of  $\xi_{\text{rot}}$  and its maximal support is given in the appendix. All we need to know here is that, using the definition (1.12), it can be written as

$$\xi_{\text{rot}}(\mathbf{x}) = \mathbf{x} \mathbf{n} - \mathbf{m} \mathbf{x}, \quad \text{where} \quad \mathbf{m}^2 = \mu^2 \mathbf{1}, \quad \mathbf{n}^2 = \nu^2 \mathbf{1}. \quad (4.1)$$

Hence,  $\mathbf{m}, \mathbf{n} \in \mathfrak{sl}(2)$  are two spacelike Minkowski vectors with lengths  $\mu$  and  $\nu$ . Depending



light cone attached to the *last point* on  $\Lambda_-$ . And vice versa, there is a white hole event horizon  $h_+$  attached to the *first point* on  $\Lambda_+$ , which separates the wormhole from the second exterior region. Inside the wormhole, we have an additional inner horizon  $c_{\pm}$ , which encloses the region that is causally connected to the singularity.

The particles themselves pass through the wormhole, from one exterior region to the other. An observer in  $\Sigma_-$  sees the particles coming from infinity, approaching each other, and falling into a black hole. Another observer in  $\Sigma_+$  sees them falling out of a white hole, separating, and disappearing to spatial infinity. But not only the lightlike world lines of the particles pass the wormhole. There are also timelike geodesics passing through, for example the central axis of the cylinder. The wormhole obviously allows an observer to pass through without hitting the singularity, and even without crossing the inner horizon. Somewhat sloppy speaking, the passage through the wormhole is quite safe, if one sticks to the region in between or close to the particles.

This is not so in the case of the standard version of the rotating BTZ wormhole, with no matter inside. Apart from the fact that this consists of a whole series of exterior regions connected by timelike wormholes, the crucial difference is that there it is not possible to pass from one exterior region to the next without crossing, or at least touching the inner horizon. The reason is that before the singular region is removed, the closed timelike curves in the quotient space fill a subset that separates the two exterior regions from each other. Hence, every curve connecting two exterior regions necessarily has to cross the chronology horizon. As this becomes the inner horizon when the singular region is taken away, it follows that every observer that passes the vacuum wormhole has to pass the inner horizon.

### The event horizons

To locate the two event horizons, we can apply the same method that we already used to find the chronology horizon. First we look for the apparent positions of the last point on  $\Lambda_-$  and the first point on  $\Lambda_+$ . Then we evolve the past, respectively the future light cones from there. From figure 5, it is quite obvious that the relevant points are  $G_2$  and  $F_1$ , for an observer located in the interior of the cylinder above  $s_1$  and below  $s_2$ , and  $G_1$  and  $F_2$  for an observer above  $s_2$  and below  $s_1$ . Using the same arguments as before, one shows, for example, that a signal can be sent from a point above  $s_1$  and below  $s_2$  to  $\Lambda_-$  if and only if it lies in the past of  $G_2$ .

The relevant pieces of the null planes with destination  $G_1$  and  $G_2$  are shown in figure 8(a). They form the black hole event horizon  $h_-$ . The subset below is the exterior region  $\Sigma_-$ . Again, the horizon is a single null plane in  $\mathcal{S}$ . The two pieces fit together correctly along the cut surfaces, because the points  $G_1$  and  $G_2$  are fixed points of the isometries  $g_2$  and  $g_1$ . The same holds for the white hole event horizon  $h_+$ , which consists of two pieces of the null planes which originate from the points  $F_1$  and  $F_2$ . This is shown in figure 8(b). Together they enclose the wormhole region  $\Omega$ , as can be seen in figure 8(c).

What is different to the inner horizon is that the event horizons reach the particles. If we

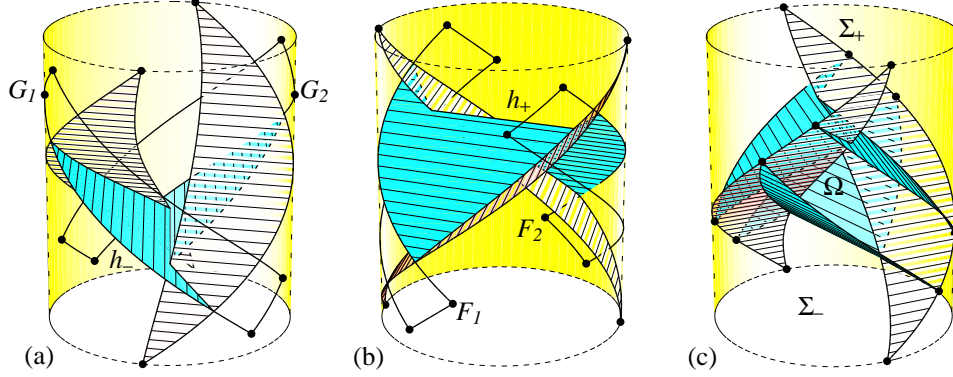


Figure 8: The black hole event horizon (a) is made out of two pieces of null planes, with destinations  $G_1$  and  $G_2$ , forming a single null plane  $h_-$  in  $\mathcal{S}$ . It emerges from a cusp, located on the spacelike geodesic connecting the particles in the moment when they fall behind it. The white hole horizon (b) consists of pieces of the null planes with origin  $F_1$  and  $F_2$ , forming a null plane  $h_+$  in  $\mathcal{S}$ . Together (c) they enclose the interior of the wormhole.

follow, for example, the null planes attached to  $G_1$  and  $G_2$  backwards in time, then at some point they hit the particles. Both particles are hit at the same time, and this is also the moment when the two null planes intersect. This can be inferred from the symmetry of our spacetime and the fact that the world lines are fixed lines of  $f_1$  and  $f_2$ . Hence, if one of the null planes hits a particle, then the other does as well, and due to the symmetry under rotations by 180 degrees the same happens to the other particle at the same time. It also follows that the two pieces of the horizon intersect along the spacelike geodesic that connects the particles at this moment.

Note that this is a *self* intersection of a single null plane in  $\mathcal{S}$ , which is due to the conical singularities on the world lines. A plane that intersects a conical singularity, which is not orthogonal to the plane, necessarily has a kink on a line that points away from the point of intersection. The horizons are exactly those null planes in  $\mathcal{S}$ , for which this kink is located on a geodesic connecting the particles. We can think of this self intersection as a cusp from where the horizon  $h_-$  emerges. If we go further back in time, then we can reach spatial infinity  $\Lambda_-$  by either sticking to one or the other side of the null planes. We are then always in the region that is causally connected to  $\Lambda_-$ . We can say that the horizon  $h_-$  is created when the particles reach a critical distance, and at the same time they fall behind it.

The same, but with the time direction reversed, happens in the second exterior region  $\Sigma_+$ . An observer sees the particles emerging from a white hole. At the same moment, the event horizon  $h_+$  degenerates to a spacelike geodesic connecting the particles, and then it disappears. The time when the black hole horizon is formed can be easily calculated. The two null planes

of which it is made of are those that arrive at the points  $G_1$  and  $G_2$  at  $t = t_G$ . As these are two antipodal points on the boundary of the cylinder, the null planes intersect in the middle of the cylinder at  $t = t_G - \pi/2 = t_A + t_{A'}$ . Similarly, one finds that the time when the white hole horizon disappears is  $t = t_F + \pi/2 = t_D - t_{A'}$ .

This can be used to compute the length  $\ell$  of the horizon. From the moment it is created the length is constant. This is because, as we just saw, the horizon is a null plane with no kinks other than the cusp from where it emerges. Immediately after its creation, the length is twice the distance between the particles. So, what we need to know is the distance between the particles. The most convenient way to compute this is to get back to the hyperbolic radial coordinate  $\chi$  on anti-de Sitter space. According to (1.1), it measures the physical distance of a point in  $\mathcal{S}_0$  from the central axis of the cylinder at  $\chi = 0$ . Due to the symmetry, the radial coordinate  $\chi$  of the points where the particles hit the horizon is the same for both particles, and the horizon length is then  $\ell = 4\chi$ .

We know how to transform the spherical coordinates back to the hyperbolic ones. Equation (1.6) tells us that

$$\cosh\left(\frac{\ell}{4}\right) = \frac{1}{\sin\theta \sin\varphi}, \quad (4.2)$$

where  $\theta$  and  $\varphi$  are the spherical coordinates of either particle one or two at the moment when the horizon is created. Let us choose particle one, whose world line  $p_1$  is defined by (2.5). The coordinate  $\varphi$  is then given by  $\cos\varphi = \tanh\delta$ , which implies that  $\sin\varphi = 1/\cosh\delta$ , and  $\theta$  is equal to  $t = t_A + t_{A'}$ . Inserting the values for  $t_A$  and  $t_{A'}$  from (3.6) and (3.13), and expressing the parameter  $\delta$  in terms of  $\mu$  and  $\nu$ , as defined in (3.5), one arrives at the simple relation

$$\ell = \mu + \nu. \quad (4.3)$$

This agrees with the result that for a non-rotating black hole formed by colliding particles, where  $\delta = 0$  and therefore  $\mu = \nu$ , the horizon length is  $\ell = 2\mu$  [6].

### The angular velocity

Not surprisingly, our wormhole also has a non-vanishing angular velocity. Let us briefly remind ourselves how this is defined [21]. As already discussed in the beginning, for an axially symmetric black hole one has a rotational Killing vector  $\xi_{\text{rot}}$ , which is uniquely defined by the condition that  $e^{2\pi\xi_{\text{rot}}} = \text{id}$ . If the black hole is also static, then there is a second Killing vector  $\xi_{\text{time}}$ , which is hypersurface orthogonal and generates time translations. It is also orthogonal to  $\xi_{\text{rot}}$ , and equal to the horizon generating Killing vector  $\xi_{\text{hor}}$ . What is meant by this is that  $\xi_{\text{hor}}$  is the Killing vector which is spacelike outside, lightlike on, and timelike inside the black hole, and whose geodesic flow lines are the light rays that travel along the horizon.

If the black hole is not static but still stationary, then the Killing vector  $\xi_{\text{time}}$  is no longer hypersurface orthogonal, and it can no longer be chosen to be orthogonal to  $\xi_{\text{rot}}$ . However, it is

still uniquely, up to rescaling, defined by the condition that  $\xi_{\text{rot}}$  and  $\xi_{\text{time}}$  should be orthogonal on  $\mathcal{J}$ , or *asymptotically orthogonal* in the sense of (1.18). The horizon is still a fixed surface of both rotations and time translations, and thus  $\xi_{\text{rot}}$  and  $\xi_{\text{time}}$  are both tangent to it. However, there is only one linear combination,

$$\xi_{\text{hor}} = \xi_{\text{time}} + \omega \xi_{\text{rot}}, \quad (4.4)$$

which is also tangent to the individual light rays spanning the horizon, and this defines the angular velocity  $\omega$  of the black hole. In asymptotically flat spacetimes,  $\xi_{\text{time}}$  can be expressed in physical units, so that  $\omega$  gets the correct dimension 1/time. In anti-de Sitter space, we can only refer to the coordinate time  $t$ . A possible way to normalize  $\xi_{\text{time}}$  is to require that on  $\mathcal{J}$  its norm is the same as that of the rotational Killing vector,  $\xi_{\text{time}}^2 = -\xi_{\text{rot}}^2$ , with respect to the conformally transformed metric (1.4). This is independent of the conformal factor, and we get the same normalization as in empty anti-de Sitter space, where  $\xi_{\text{time}} = \partial_t$  and  $\xi_{\text{rot}} = \pm \partial_\theta$ .

Now, we have the expression (4.1) for the rotational Killing vector  $\xi_{\text{rot}}$ , and from (1.18) we know how to construct an asymptotically orthogonal Killing vector  $\xi_{\text{time}}$ , namely

$$2\pi \xi_{\text{rot}}(\mathbf{x}) = \mathbf{x} \mathbf{n} - \mathbf{m} \mathbf{x} \quad \Rightarrow \quad 2\pi \xi_{\text{time}}(\mathbf{x}) = -\mathbf{x} \mathbf{n} - \mathbf{m} \mathbf{x}. \quad (4.5)$$

Up to a sign,  $\xi_{\text{time}}$  is determined by the condition that  $\xi_{\text{time}}^2 = -\xi_{\text{rot}}^2$ . The sign is chosen such that  $\xi_{\text{time}}$  is pointing towards the future, with  $\mathbf{m}$  and  $\mathbf{n}$  given by (A.5). Inserting this into (4.4), we get

$$2\pi \xi_{\text{hor}}(\mathbf{x}) = \mathbf{x} \mathbf{n} (\omega - 1) - (\omega + 1) \mathbf{m} \mathbf{x}. \quad (4.6)$$

What we have to find is that value of  $\omega$  for which  $\xi_{\text{hor}}$  is tangent to the light rays on the horizon. This can be done without explicitly calculating  $\xi_{\text{hor}}$  on the horizon. We know that the horizon is made out of pieces of null planes. We also know that these null planes are fixed surfaces of the Killing vectors  $\xi_{\text{rot}}$  and  $\xi_{\text{time}}$ , and hence of  $\xi_{\text{hor}}$  for any given value of  $\omega$ . Among all the possible linear combination of  $\xi_{\text{rot}}$  and  $\xi_{\text{time}}$ , we have to find that one which also has the individual light rays as fixed lines.

In section 1 we saw that the condition (1.29) for the Killing vector  $\xi_{\text{hor}}$  to have a family of fixed light rays is that the Minkowski vectors appearing to the left and to the right of  $\mathbf{x}$  in the definition (4.6) are either lightlike or spacelike and of the same length. This leads to the condition that

$$\mathbf{n}^2 (\omega - 1)^2 = \mathbf{m}^2 (\omega + 1)^2 \quad \Rightarrow \quad \nu (\omega - 1) \pm \mu (\omega + 1) = 0. \quad (4.7)$$

There are two solutions, namely

$$\omega = \frac{\nu - \mu}{\nu + \mu}, \quad \tilde{\omega} = \frac{\nu + \mu}{\nu - \mu}. \quad (4.8)$$

Now, why do we get two solutions, and what is the correct one? First of all, the condition only tells us that there is *some* family of fixed light rays. This need not be the event horizon, it can

also be the inner horizon, which is a second fixed null plane of both  $\xi_{\text{time}}$  and  $\xi_{\text{rot}}$ . It is however easy to see which is the correct one.

For  $\xi_{\text{hor}}$  to be timelike outside the horizon, and thus in particular on  $\mathcal{J}$ , where  $\xi_{\text{time}}$  and  $\xi_{\text{rot}}$  are unit timelike and spacelike vectors, we must have  $|\omega| < 1$ . This implies that the first solution  $\omega$  must be the correct one. It also gives the correct limit  $\omega = 0$  for  $\mu = \nu$ , which is the case when the particles collide and a static black hole is formed. We shall discuss this in more detail below. The second solution  $\tilde{\omega} = 1/\omega$  is the angular velocity of the inner horizon. It goes to infinity in the static case, which is also quite reasonable as we shall see.

Like every rotating black hole, our wormhole also has an ergosphere. That is, a region of spacetime surrounding the event horizon where it is impossible to stand still, with respect to the generating Killing vector  $\xi_{\text{time}}$  of time translations. To see this, we have to show that  $\xi_{\text{time}}$  is spacelike on the event horizon, and thus already in a finite neighbourhood of the horizon. Let us compute the norm of both  $\xi_{\text{time}}$  and  $\xi_{\text{rot}}$  on the horizon. Using the formula (1.17), we find that

$$4\pi^2 \xi_{\text{time}}^2 = \frac{1}{2} \text{Tr}(\mathbf{n}^2 + \mathbf{m}^2 + 2\mathbf{x}^{-1}\mathbf{m}\mathbf{x}\mathbf{n}), \quad 4\pi^2 \xi_{\text{rot}}^2 = \frac{1}{2} \text{Tr}(\mathbf{n}^2 + \mathbf{m}^2 - 2\mathbf{x}^{-1}\mathbf{m}\mathbf{x}\mathbf{n}). \quad (4.9)$$

On the other hand, we know that the vector

$$2\pi \xi_{\text{hor}} = -\frac{2\mu\mathbf{x}\mathbf{n} + 2\nu\mathbf{m}\mathbf{x}}{\mu + \nu}, \quad (4.10)$$

obtained by inserting the correct value for  $\omega$  into (4.4), is lightlike on the event horizon, and thus

$$\pi^2 (\mu + \nu)^2 \xi_{\text{hor}}^2 = \frac{1}{2} \text{Tr}(\mu^2\mathbf{n}^2 + \nu^2\mathbf{m}^2 + 2\mu\nu\mathbf{x}^{-1}\mathbf{m}\mathbf{x}\mathbf{n}) = 0. \quad (4.11)$$

Using that  $\mathbf{m}^2 = \mu^2\mathbf{1}$  and  $\mathbf{n} = \nu^2\mathbf{1}$ , this tells us that on the event horizon we have  $\text{Tr}(\mathbf{x}^{-1}\mathbf{m}\mathbf{x}\mathbf{n}) = -2\mu\nu$ . Inserting this into (4.9), we find that

$$4\pi^2 \xi_{\text{time}}^2 = (\nu - \mu)^2, \quad 4\pi^2 \xi_{\text{rot}}^2 = (\nu + \mu)^2. \quad (4.12)$$

Hence, both  $\xi_{\text{rot}}$  and  $\xi_{\text{time}}$  are spacelike on the event horizon. The only exception is the static case, where  $\mu = \nu$  and therefore  $\xi_{\text{time}}$  is lightlike. In this case, there is of course no ergosphere.

We can also define a generating Killing vector of the inner horizon, which is obtained by just replacing  $\omega$  with  $\tilde{\omega} = 1/\omega$ , or  $\mu$  with  $-\mu$ . Repeating the same calculation gives that on the inner horizon we have

$$4\pi^2 \xi_{\text{time}}^2 = (\nu + \mu)^2, \quad 4\pi^2 \xi_{\text{rot}}^2 = (\nu - \mu)^2. \quad (4.13)$$

So, for generic values of  $\mu$  and  $\nu$ , both  $\xi_{\text{rot}}$  and  $\xi_{\text{time}}$  are also spacelike on the inner horizon. In particular,  $\xi_{\text{rot}}$  is not yet lightlike, which means that the singularity is further behind the inner horizon. The only exception is again the static case, where  $\xi_{\text{rot}}$  is lightlike on the inner horizon. In this case, it consists of a family of closed lightlike geodesics, and this is already the singularity. This is also the reason why the angular velocity  $\tilde{\omega}$  of the inner horizon diverges in the static case, whereas the angular velocity of the event horizon goes to zero. The generating Killing vector of the inner horizon coincides with  $\xi_{\text{rot}}$ , whereas the generating Killing vector of the event horizon is  $\xi_{\text{time}}$ .

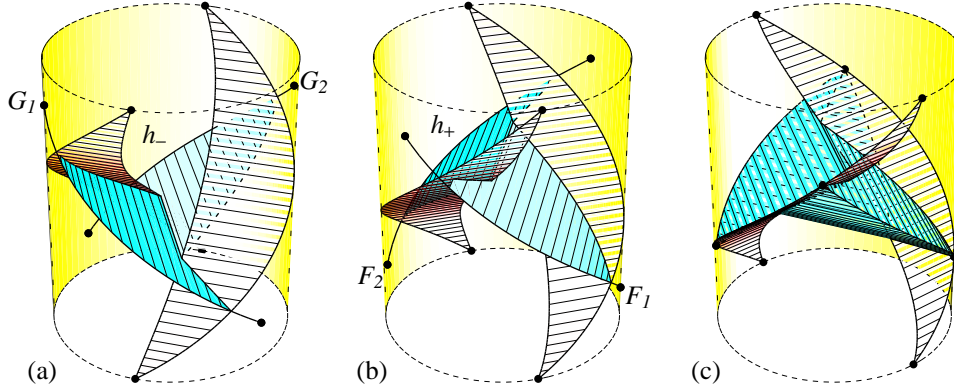


Figure 9: The extremal, or lightlike wormhole with  $0 = \mu < \nu$ . The rectangles of figure 5 on the boundary are degenerate. There are no closed timelike curves, and the singularity consists of a single closed light ray on  $\mathcal{J}$ . There is no inner horizon, but the event horizons  $h_{\pm}$  are still there, consisting of pieces of null planes attached to the points  $G = H$ , and  $E = F$ .

### Extremal and static black holes

To complete the discussing of the wormhole spacetime, let us consider some limits. We have two parameters  $0 < \mu < \nu$ , which we can think of as specifying the properties of the wormhole. They determine the horizon length (4.3) and the angular velocity (4.8). They are related to the parameters  $\delta$  and  $\epsilon$  by (3.5), describing the relative motion of the particles. There are two limits we can take. For  $0 < \mu = \nu$ , the angular velocity of the black hole vanishes. In this case we have  $\delta = 0$ , which means that the particles collide. The other special situation is  $0 = \mu < \nu$ . This is the case when the relevant function of the energy and the distance of the particles has just reached the threshold,  $e^{\delta} = \tan \epsilon$ . And finally, we can also consider the very special situation  $0 = \mu = \nu$ .

Let us consider the second case first. For  $0 = \mu < \nu$ , we have an *extremal* black hole. From (3.6) we infer that  $t_A = t_B$  and  $t_C = t_D$ , which means that the region  $\Gamma$  of closed timelike curves on  $\mathcal{J}$ , as shown in figure 4, is degenerate to a single closed light ray. There are no closed timelike curves at all on  $\mathcal{J}$ , and consequently also no closed timelike curves in  $\mathcal{S}$ . This also follows from the condition (A.20) for closed timelike curves derived in the appendix. If we take the limit  $\mu \rightarrow 0$  with fixed  $\nu > 0$ , then the chronology horizon of the Gott universe shrinks and finally disappears at  $\mathcal{J}$ . But we can still consider the remaining closed light rays on  $\mathcal{J}$  as a singularity, splitting  $\mathcal{J}$  into two disconnected infinities  $\Lambda_-$  and  $\Lambda_+$ .

Evolving the past and future light cones from the apparent positions of the last point on  $\Lambda_-$  and the first point on  $\Lambda_+$ , we find the black hole and the white hole horizon, enclosing the interior of the wormhole. As indicated in figure 9, the rectangles  $\tilde{\Gamma}$  constructed in figure 5 are



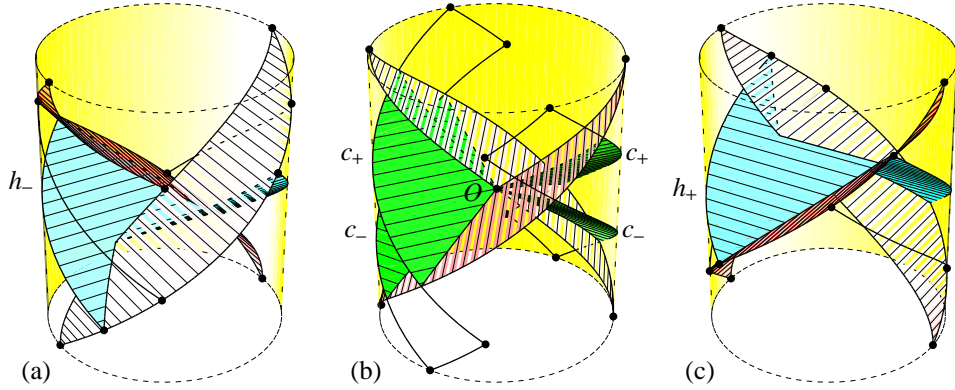


Figure 10: A static black hole formed by colliding particles with  $0 < \mu = \nu$ . The chronology horizon reaches the world lines in the moment of collision  $O$ . When interpreted as a Gott universe, this spacetime is geodesically incomplete. When the singular region, which coincides with the interior of the chronology horizon, is removed, then the wormhole closes and the spacetime falls apart into a black hole and a white hole.

also degenerate, and the origins and destinations of the event horizons  $F$  and  $G$  now coincide with the points  $E$  and  $H$ . As a consequence, the event horizons meet at the boundary of the cylinder, and there is no room any more for an inner horizon and a singularity inside  $S$ . The wormhole is infinitely large, because the singularity is infinitely far away. It has also reached its maximal angular velocity  $\omega = 1$ .

For  $0 < \mu = \nu$  we have the opposite situation. The angular velocity vanishes, and we expect the wormhole to be static. In this case, we also have  $\delta = 0$ , which means that the particles collide at  $t = \pi/2$  in the centre of the cylinder. This process has already been studied in [6], with the result that two colliding particles form a static black hole, but not a wormhole. Indeed, if we look at the equations (3.14), and take into account that for  $\mu = \nu$  we have  $t_P = t_{P'}$  for all the points  $P = A, B, C, D$  on the cuts, then we find that  $t_E = 0$  and  $t_H = \pi$ . These are the origins and destinations of the null planes that form the chronology horizon.

If their distance in time is  $\pi$ , then the null planes emerging from there meet at  $t = \pi/2$  in the centre of the cylinder. But this is also the point  $O$  where the particles collide, as shown in figure 10(b). Hence, what happens in the special case of colliding particles is that in the moment of collision they also hit the chronology, or inner horizon. Even worse, this is already the singularity, which has been defined to be the surface where  $\xi_{\text{rot}}$  is lightlike. On the other hand, we have seen that in the static case the angular velocity of the inner horizon is infinite, which means that  $\xi_{\text{rot}}$  is also the generating Killing vector of the inner horizon. Hence, the inner horizon coincides with the singularity and it touches the particles in the moment of collision.

This agrees very nicely with the result of [6], where it has been shown that the only way to avoid closed timelike curves after the collision of the particles is to assume that the particles stick together and form a tachyonic object, which is interpreted as a future singularity of a black hole. Here we have the same situation. Every timelike curve that enters the event horizon necessarily ends on the inner horizon, and thus on the singularity. Moreover, the singularity also emerges, in a sense, from the point of collision of the two particles. If we take away the singular region, then the spacetime falls apart into two disconnected components, a black hole and its white hole counterpart. So, we agree with the previous result, and we also find the same horizon length of  $\ell = 2\mu$ .

We can think of the generalized Gott universe, with the closed timelike curves not being removed, as a possible extension of the static black hole *beyond* the singularity. Such an extension necessarily contains closed timelike curves. It was the ADM like formulation used in the previous work to describe the colliding particles, which prevented us from seeing how such an extension looks like. Now we have an explicit representation in form of a generalized Gott universe. There remains, however, one somewhat peculiar and rather unexpected feature of the spacetime  $\mathcal{S}$  with  $\mu = \nu$ . Obviously, although the infalling particles have no angular momentum, the spacetime shown in figure 10 has an inherent orientation.

The closed timelike curves wind around the particles in one direction but not in the other. This suggests that the extension of the static black hole is not unique. There must be at least a second one, with opposite orientation. We can also see this when we look more closely at the scattering process of the two particles. When they hit each other, it is not clear in which direction they should continue afterwards. Here we assumed that the particles move on as if they had passed each other on the right. We can also take the limit from the left. Then we obtain an alternative extension of the static black hole, with the opposite orientation. The third possibility is that the particles stick together. This is the only way to avoid the closed timelike curves [6].

If there are several possible generalized Gott universes, which are all extensions of the static black hole, then neither of them can be geodesically complete. So far, we haven't considered this problem at all. Actually, all our spacetimes might be geodesically incomplete. That is, before the singular region is removed, since afterwards they are incomplete anyway. If this is the case, then we probably miss some interesting features. There might be a second singularity, for example. Fortunately, it turns out that all universe constructed here are geodesically complete, except for those with  $\mu = \nu$ . The proof is given in the appendix. In the static case, there are geodesics that wind around the particles infinitely many times, such that with each winding their affine length decreases. As a result, the total length of such a geodesic converges.

The problem is of the same type as in the well known case of the *Misner universe* [4], which is sketched in figure 11. It is a simple two or higher dimensional locally flat and symmetric spacetime with a singularity in the future, similar to that of a static BTZ black hole. It can be extended beyond the singularity in two different ways. Both contain closed timelike curves, and both have an inherent orientation. The closed timelike curves wind either in one or the other

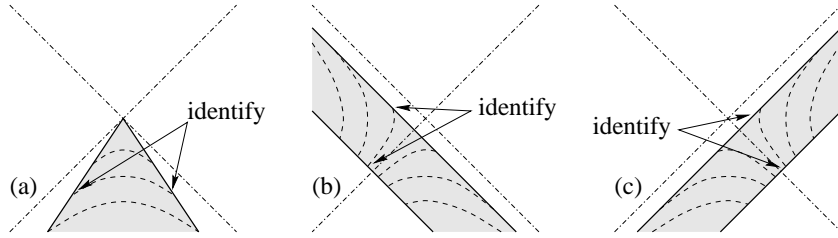


Figure 11: The Misner universe (a) is a wedge in the past of the origin of 1 + 1 dimensional Minkowski space, with the faces identified by the action of a boost. It has a big crunch like singularity at the origin. It is isometric to the quotient space of the interior of the past light cone with respect to the given boost. There are two possible extensions, either including the left (b) or the right (c) spacelike region and then taking the quotient. Both contain closed timelike curves, and both are still incomplete. To get a geodesically complete spacetime, one has to include the whole Minkowski space, but then the quotient is no longer a Hausdorff space.

direction. Both extensions are still geodesically incomplete. It is not possible to construct a geodesically complete spacetime from the Misner universe which is at the same time a proper manifold. The same is happening here as well. There are several possible extensions of the static black hole, but none of them is geodesically complete.

Finally, let us also consider the extremal static case  $0 = \mu = \nu$ . This has also been discussed in [6]. At first sight, there seems to be a contradiction. For the extremal wormhole we found that there is no inner horizon and the singularity is infinitely far away. For the static one it even reaches the particles. The solution is that in the extremal static case there are indeed no closed timelike curves, but there is a family of closed lightlike geodesics. The inner horizon is degenerate to a null plane, with no interior, but it still reaches the particles in the moment of collision. Moreover, it also coincides with the event horizons, which means that there is no interior of the wormhole, and the horizon length is zero. Again, all this agrees with the previous results.

To summarize, it seems that the actually rotating black hole has a much simpler structure than the static one. This is probably a bit surprising, because usually the situation is the other way around. There are very elegant ways to construct rotating *vacuum* black holes [14, 15], with no infalling matter, but, as compared to the static ones, it is much harder to visualize them. Usually, one only has a geometric description of their covering spaces as subsets of anti-de Sitter space, but unless the angular velocity vanishes one cannot identify a primitive patch from which they can be constructed by cutting and gluing.

The effect of the particles seems to be that they cut away certain pieces of these spacetimes, as described in the last section of [6], such that a visualization by cutting and gluing becomes possible. It is also the presence of the particles, and in particular the fact that they are massless,

which makes it possible to study a single wormhole, instead of a periodic sequence. If the particles would not emerge from  $\mathcal{J}$  at some time and disappear at a later time, then the whole spacetime would become periodic in  $t$  with a period of  $\pi$ . Like in the maximally extended rotating vacuum BTZ black hole, we would then get a whole sequence of wormholes connecting a series of external universes.

## Acknowledgements

We would like to thank Ingemar Bengtsson and Jorma Louko for many valuable discussions, and the Albert Einstein Institute in Potsdam for hospitality.

## Appendix

Here we want to give some technical details which are not necessary to understand the description of our spacetime, but which are needed to prove some of its properties. There are basically three open problems, namely the definition of the rotational Killing vector, the proof of geodesic completeness, and we have to show that there is only one region of closed timelike curves.

### The rotational Killing vector

Consider the isometries  $g_1$  and  $g_2$  on anti-de Sitter space, as defined in (3.7). On the group manifold, they can be written as

$$g_1 : \quad x \mapsto (\gamma_0 \mathbf{u}_1)^{-1} x (\gamma_0 \mathbf{v}_1), \quad g_2 : \quad x \mapsto (\gamma_0 \mathbf{u}_2)^{-1} x (\gamma_0 \mathbf{v}_2), \quad (\text{A.1})$$

with the group elements  $\mathbf{u}$  and  $\mathbf{v}$  given by (2.3) and (2.4). The first step is to define two Killing vectors  $\xi_1$  and  $\xi_2$  such that  $g_1$  and  $g_2$  are their flows. To do this, we have to write the group elements appearing in (A.1) as exponentials. It follows from

$$\text{Tr}(\gamma_0 \mathbf{u}_1) = \text{Tr}(\gamma_0 \mathbf{u}_2) = -2 \cosh(\mu/2), \quad \text{Tr}(\gamma_0 \mathbf{v}_1) = \text{Tr}(\gamma_0 \mathbf{v}_2) = -2 \cosh(\nu/2), \quad (\text{A.2})$$

that all of them are hyperbolic or, for  $\mu$  or  $\nu$  equal to zero, parabolic elements of  $\text{SL}(2)$ . In any case, they can be *uniquely* written as exponentials, such that

$$\gamma_0 \mathbf{u}_1 = -e^{\mathbf{m}_1/2}, \quad \gamma_0 \mathbf{v}_1 = -e^{\mathbf{n}_1/2}, \quad \gamma_0 \mathbf{u}_2 = -e^{\mathbf{m}_2/2}, \quad \gamma_0 \mathbf{v}_2 = -e^{\mathbf{n}_2/2}, \quad (\text{A.3})$$

where  $\mathbf{m}, \mathbf{n} \in \mathfrak{sl}(2)$  are either spacelike or lightlike Minkowski vectors, with

$$\mathbf{m}^2 = \mu^2 \mathbf{1}, \quad \mathbf{n}^2 = \nu^2 \mathbf{1}. \quad (\text{A.4})$$

Explicitly, we find that

$$\mathbf{m}_{1,2} = -\mu \frac{\gamma_0 \pm \cosh(\mu/2)\gamma_1}{\sinh(\mu/2)}, \quad \mathbf{n}_{1,2} = -\nu \frac{\gamma_0 \mp \cosh(\nu/2)\gamma_1}{\sinh(\nu/2)}. \quad (\text{A.5})$$

The Killing vectors with the required properties  $g_1 = e^{\pi\xi_1}$  and  $g_2 = e^{\pi\xi_2}$  are defined such that

$$2\pi \xi_1(\mathbf{x}) = \mathbf{x} \mathbf{n}_1 - \mathbf{m}_1 \mathbf{x}, \quad 2\pi \xi_2(\mathbf{x}) = \mathbf{x} \mathbf{n}_2 - \mathbf{m}_2 \mathbf{x}, \quad (\text{A.6})$$

where, as explained in section 1,  $\mathbf{x}$  is understood as an  $\text{SL}(2)$  valued function on anti-de Sitter space, so that  $\xi_1$  and  $\xi_2$  become vector fields on  $\mathcal{S}_0$ .

The rotational Killing vector  $\xi_{\text{rot}}$  on  $\mathcal{S}$  will be defined piecewise. First we have to specify its support. Consider the flow lines of  $\xi_1$  starting off from the surface  $s_2$ . All these flow lines end up on the surface  $s_1$ . This is because  $s_1$  is a fixed surface of  $f_1$ , and therefore we have  $e^{\pi\xi_1}(s_2) = g_1(s_2) = f_1(r(s_2)) = f_1(s_1) = s_1$ . It is also not difficult to find out in which direction these flow leave  $s_2$ , and from which direction they arrive at  $s_1$ . They either leave the lower face of  $s_2$  and arrive at the upper face of  $s_1$  or vice versa. However, the latter is excluded. This can be seen in figure 5. If the flow lines of  $\xi_1$  start off from the upper face of  $s_2$  and reach  $s_1$  from below, then they had to cross the fixed right moving light rays  $A'_2C'_1$  and  $B'_2D'_1$  of  $g_1$ .

But this is impossible, because  $g_1$  is the flow of  $\xi_1$ . Hence, the flow lines of  $\xi_1$  connect the lower face of  $s_2$  with the upper face of  $s_1$ . Similarly, the flow lines of  $\xi_2$  connect the lower face of  $s_1$  with the upper face of  $s_2$ . Let us denote the regions of anti-de Sitter space filled by these flow lines by

$$\Pi_1 = \bigcup_{\tau \in [0, \pi]} e^{\tau\xi_1}(s_2), \quad \Pi_2 = \bigcup_{\tau \in [0, \pi]} e^{\tau\xi_2}(s_1). \quad (\text{A.7})$$

They are bounded by the cut surfaces  $s_1$  and  $s_2$ , the boundary  $\mathcal{J}$  of the cylinder, and the flow lines connecting the world lines of the particles. We have sketched the situation in figure 12(a). Obviously,  $\Pi = \Pi_1 \cup \Pi_2$  can also be regarded as a subset of  $\mathcal{S}$ , we only have to glue the two parts together appropriately along the cut surfaces. Their union has the shape of a torus, with the world lines of the particles sitting on its inner boundary. This subset of  $\mathcal{S}$  is the maximal support of the rotational Killing vector  $\xi_{\text{rot}}$ , which is defined to be

$$\xi_{\text{rot}}|_{\Pi_1} = \xi_1, \quad \xi_{\text{rot}}|_{\Pi_2} = \xi_2. \quad (\text{A.8})$$

What we have to show is that this is indeed a Killing vector, which is obvious everywhere except on the cut surfaces, and that its flow lines are closed, such that  $e^{2\pi\xi_{\text{rot}}} = \text{id}$ . All this can be inferred from the relations

$$g_1 = f_1 \circ g_2 \circ f_1^{-1}, \quad g_2 = f_2 \circ g_1 \circ f_2^{-1}, \quad (\text{A.9})$$

between the isometries that define the Killing vectors and the transition function on the cut surfaces. They imply that

$$f_1^*(\xi_2) = \xi_1, \quad f_2^*(\xi_1) = \xi_2, \quad (\text{A.10})$$

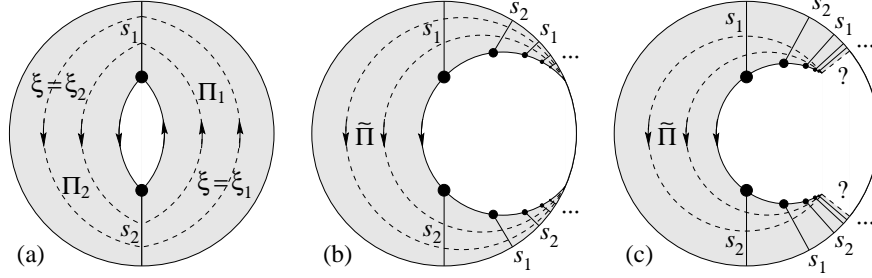


Figure 12: A schematic picture (a) of the support  $\Pi$  of the rotational Killing vector  $\xi_{\text{rot}}$ . The covering space  $\tilde{\Pi}$  is obtained by attaching infinitely many copies of  $\Pi_1$  and  $\Pi_2$  to each other, which are isometric to the subsets  $g_2^n(\Pi_2)$ ,  $n \in \mathbb{Z}$ . If  $g_2$  has no fixed light rays other than those on the boundary (b), then the spacetime  $\mathcal{S}$  is geodesically complete. Otherwise (c) it is incomplete.

where  $f^*$  denotes the push forward of vectors induced by  $f$ . Now, consider the vector  $\xi_{\text{rot}}$  in the neighbourhood of the cut surface  $s_1$ . We saw that the region below  $s_1$  is part of  $\Pi_2$ , and that above  $s_1$  is part of  $\Pi_1$ . Hence, we have that  $\xi_{\text{rot}} = \xi_2$  below and  $\xi_{\text{rot}} = \xi_1 = f_1^*(\xi_2)$  above  $s_1$ . On the other hand,  $f_1$  is the isometry that relates an object defined below  $s_1$  to the same object defined above  $s_1$ , and therefore  $\xi_1$  represents the same Killing vector above  $s_1$  as  $\xi_2$  does below  $s_1$ . Similarly, one shows that  $\xi_{\text{rot}}$  is well defined on the other cut surface  $s_2$ .

To prove that the flow lines are closed and  $e^{2\pi\xi_{\text{rot}}} = \text{id}$ , it is sufficient to show that this is the case for at least one point on every flow line. Let us consider the points on  $s_1$ . Starting from a point  $P$  on the lower face of  $s_1$ , which is part of  $\Pi_2$ , we follow the flow line of  $\xi_{\text{rot}} = \xi_2$  to  $e^{\pi\xi_2}(P) = g_2(P)$  on the upper face of  $s_2$ . This is identified with  $f_2^{-1}(g_2(P)) = r(P) = Q$  on the lower face of  $s_2$ . From there we follow the flow line of  $\xi_{\text{rot}} = \xi_1$  to  $e^{\pi\xi_1}(Q) = g_1(Q)$  on the upper face of  $s_1$ , which is then identified with  $f_1^{-1}(g_1(Q)) = r(Q) = P$ . Hence, we are back to where we started after a rotation by  $2\pi$ .

### Geodesic completeness

To prove that our generalized Gott universe is geodesically complete, we have to show that, given a start point and a tangent vector of a geodesic somewhere in  $\mathcal{S}$ , then it can always be extended arbitrarily far into the direction of the given vector. In other words, we have to check that the maximally extended geodesic in  $\mathcal{S}$  with the given initial conditions has an infinite total length, measured in units of the given tangent vector. The most convenient way to do this is to consider a series of different cases, distinguished by the way in which the geodesic intersects with the cut surfaces  $s_1$  and  $s_2$ .

To avoid a too complicated classification, we use the following convention regarding the

conical singularities on the world lines. Whenever a geodesic hits one of the world lines, then there are two possible extensions. We can either take a limit from the left or from the right. That is, we can extend the geodesic as if it had passed the particle on the left or on the right. We regard them as two different geodesics, and depending on which side it has passed the world line, it either intersects with the cut surface attached to that world line or not. Hence, it either belongs to one of the classes defined below or to another.

The first and simplest class to be considered consists of those geodesics in  $\mathcal{S}$  that, when maximally extended into one direction, intersect only finitely many times, or not at all, with the cut surfaces. These are certainly complete, because after the last intersection they behave like geodesics in anti-de Sitter space, and this is of course geodesically complete. Another simple class of geodesics are those that are, from the very beginning or after hitting a world line of a particle, tangent to one of the cut surfaces. They are necessarily lightlike or spacelike. The lightlike ones are exactly those that span the null half planes  $s_1$  and  $s_2$ , and these are obviously complete.

The spacelike ones either extend to  $\mathcal{J}$  without leaving the cut surfaces again, and are therefore also complete. Or, they hit the world line and leave the cut surface, in which case we can drop a finite piece and consider them as belonging to one of the other classes. So, actually only those geodesics are of interest which intersect infinitely many times with the cut surfaces. We know already that at least one such geodesic exists, namely the closed spacelike geodesic that forms the cusp of the inner horizon. Since this circle has a finite circumference, it follows that its total length is infinite. What is common to all such geodesics is that they intersect the two cut surfaces alternately.

This is simply because no geodesic in anti-de Sitter space intersects a null plane twice. But in which direction do they intersect with the cut surfaces? It is clear that a timelike or lightlike geodesic always intersects the cut surfaces into the same direction. That is, a future pointing timelike or lightlike geodesic necessarily hits the lower face and continues from the upper face. For a past pointing geodesic it is the other way around. A spacelike geodesic can however leave the upper face of one cut surface and hit the upper face of the other cut surface, or similarly leave the lower face of one cut surface and hit the other lower face. It turns out that if it does so infinitely many times, then it is complete.

To see this, we have to show that there is a finite minimal length of a spacelike geodesic that connects the two upper faces of the cut surface, respectively the two lower faces. It should be clear from figure 3 that for both the start and end point of any geodesic that connects the upper face of  $s_1$  with that of  $s_2$  we must have  $t \geq \pi/2$ . If we extend to two null half planes to become full planes, then they intersect at  $t = \pi/2$ , and it is only the part above the intersection where the upper faces point towards each other. Similarly, if a spacelike geodesic connects the two lower faces, then we must have  $t \leq \pi/2$  for both the start and the end point.

It is not very difficult to compute the length of a general spacelike geodesic in anti-de Sitter space, connecting two points represented by the group elements  $x, y \in \text{SL}(2)$ . If  $y = \mathbf{1}$  and  $x = e^{d\mathbf{n}}$ , where  $\mathbf{n} \in \mathfrak{sl}(2)$  is a unit spacelike vector, then the length of the geodesic is  $d$ ,

and thus  $\text{Tr}(\boldsymbol{x}) = 2 \cosh d$ . Using that  $\boldsymbol{x} \mapsto \boldsymbol{x}\boldsymbol{y}^{-1}$  is an isometry, it follows that the length  $d$  of a geodesic connecting  $\boldsymbol{x}$  and  $\boldsymbol{y}$  is given by  $\text{Tr}(\boldsymbol{x}\boldsymbol{y}^{-1}) = 2 \cosh d$ . Using the explicit representation of the group elements (1.25) corresponding to points  $(t, \varphi)$  on the null plane  $s_1$ , and a similar relation for points  $(t', \varphi')$  on the null plane  $s_2$ , which is obtained by replacing  $\gamma_1$  with  $-\gamma_1$  and  $\gamma_2$  with  $-\gamma_2$ , one can easily show that  $d \geq 2\delta$ .

This holds for both  $t, t' \geq \pi/2$  and  $t, t' \leq \pi/2$ , and under the condition that  $\cos \varphi \geq \tanh \delta$  and  $\cos \varphi' \geq \tanh \delta$ , which defines the parts of the null planes that actually form the cut surfaces. This is quite reasonable, because  $2\delta$  is the distance between the particles in the moment of closest approach, which is achieved at  $t = \pi/2$ . Note, however, that this is not the *minimal* distance between the particles. There are points on the world line which are lightlike separated, for example, but for them we have to choose the time coordinates such that either  $t < \pi/2 < t'$  or vice versa. In any case, a spacelike geodesic that connects the two upper faces or the two lower faces has a length of at least  $2\delta$ .

If any spacelike geodesic has infinitely many such pieces, then it is obviously complete, because it has an infinite proper length. Hence, all what remains to be shown is that all those geodesics are complete which intersect the two cut surfaces alternately and, probably after some finite number of intersections, always into the same direction. That is, they either always hit the surfaces from below and continue from above, or vice versa. It is sufficient to consider the first case only. The second is analogous, just with the time direction reversed, because  $\mathcal{S}$  is invariant under a suitable chosen time inversion, combined with a parity transformation. So, let  $\lambda$  be such a geodesic, and split it into pieces  $\lambda_n$  connecting the upper face of one cut surface with the lower face of the other cut surface.

To show that  $\lambda$  is complete, we map it isometrically onto a geodesic in anti-de Sitter space  $\mathcal{S}_0$ , and show that it converges to a point on  $\mathcal{J}_0$ . We are not going to give the full technical details of the proof here, which is completely straightforward and very similar to the construction of the covering space of the singular region in section 3. The basic idea is the following. We start from a piece  $\lambda_0$  connecting the upper face of  $s_2$  with the lower face of  $s_1$ . This is a piece of a geodesic in  $\mathcal{S}$ , but we may as well regard it as a piece of a geodesic in  $\mathcal{S}_0$ . The next piece of the geodesic in  $\mathcal{S}$  is  $\lambda_1$ , which connects the upper face of  $s_1$  with the lower face of  $s_2$ .

The continuation of the same geodesic in  $\mathcal{S}_0$  is  $f_1^{-1}(\lambda_1)$ . It starts from a point on the null half plane  $s_1$  and ends on  $f_1^{-1}(s_2) = g_2^{-1}(s_1)$ . The next piece is  $\lambda_2$  in  $\mathcal{S}$ , and it is mapped onto  $f_1^{-1}(f_2^{-1}(\lambda_2))$ , which is the continuation of the geodesic in  $\mathcal{S}_0$ . Its end point lies on the null half plane  $f_1^{-1}(f_2^{-1}(s_1)) = g_2^{-2}(s_1)$ . Continuing this way, it is not difficult to see that we obtain a geodesic in anti-de Sitter space with a series of points on the null half planes  $g_2^{-n}(s_1) = g_2^{-n-1}(s_2)$ . The crucial question is what happens to them in the limit  $n \rightarrow \infty$ . Again, it is most convenient to look at the conformal boundary first.

In figure 13, we have sketched the flow lines of  $\xi_2$ , which is the generating Killing vector of  $g_2$ . The region between the two bold lines is the outer boundary of  $\Pi_2$ , where the rotational Killing vector is  $\xi_{\text{rot}} = \xi_2$ . Continuing the flow lines beyond the cuts up to the fixed points, which we constructed in figure 5, we can see what the series of images  $g_2^{-n}(s_1) = g_2^{-n-1}(s_2)$



of the cuts looks like. For  $n \rightarrow \infty$ , they converge to the fixed line  $KGH$ , and for  $n \rightarrow -\infty$ , which we have to consider if we extend our geodesic into the opposite direction, they converge to the fixed line  $EFL$ . Note that the fixed points  $K$  and  $L$  could not be seen in figure 5 because they are outside the time interval  $0 < t < \pi$ .

In any case, what we see is that on the boundary of the cylinder, the images of the cuts  $s_1$  and  $s_2$  converge to a pair of fixed light rays on  $\mathcal{J}_0$ . What does this mean for the null half planes  $g_2^{-n}(s_1) = g_2^{-n-1}(s_2)$  inside the cylinder? Obviously, they have to converge to the null plane with origin  $K$  and destination  $H$  for  $n \rightarrow \infty$ , respectively to the null plane with origin  $E$  and destination  $L$  for  $n \rightarrow -\infty$ . Note that  $K$  and  $H$ , as well as  $E$  and  $L$  are antipodal points on  $\mathcal{J}_0$ . Moreover, but this is not of particular importance here, these are also the null planes that form the inner horizon, which we already know to be fixed surfaces of  $g_2$ . But now, the surfaces  $s_1$  and  $s_2$  are null *half* planes, so what is also important to know is what happens to the images of the world lines  $g_2^{-n}(p_1) = g_2^{-n-1}(p_2)$ .

There are three possible cases. One possibility, which is shown in figure 12(b), is that they also converge to the fixed light rays  $KGH$  and  $EFL$  of  $\mathcal{J}_0$ . Then we are finished, because this immediately implies that also the points on the geodesic under consideration converge to  $\mathcal{J}_0$ . We can also say that in this case the null half planes actually disappear in the limit  $n \rightarrow \infty$ . Another way to explain this is to consider the shaded region of figure 12(b) as the covering space  $\tilde{\Pi}$  of the support of the rotational Killing vector. Obviously, every geodesic in this region either reaches  $\mathcal{J}$ , and is thus complete, or it hits the inner boundary of  $\Pi$  and continues in the complement of  $\Pi$  in  $\mathcal{S}$ , which is a simply connected subset of anti-de Sitter space. Hence, in neither part of  $\mathcal{S}$  a geodesic can get lost.

A second possible scenario is that the images  $g_2^{-n}(p_1) = g_2^{-n-1}(p_2)$  of the world lines converge to the boundary of the cylinder, but on the opposite side of the limiting null plane. In this case, we would say that the null half planes become full planes in the limit. This however is excluded, for the following reason. As can be seen in figure 13, the flow lines on which the origins and destinations of the null planes approach their fixed points, that is, the uppermost and the lowermost flow lines shown, are spacelike. This implies that the null planes emerging from two points very close to each other on these lines will always overlap. Hence, for large  $n$  the surfaces  $g_2^{-n-1}(s_1)$  and  $g_2^{-n}(s_1) = g_2^{-n-1}(s_2)$  would overlap. However,  $g_2^{-n-1}$  is an isometry, and thus  $s_1$  and  $s_2$  would also overlap, and this is not the case.

The only case that remains is the one shown in figure 12(c). The world lines converge to light rays inside the cylinder, so that in the limit the null half planes remain half planes. In this case, the spacetime would be geodesically incomplete, because a geodesic that approaches the limiting null half plane has a finite length, but cannot be extended further. Using the interpretation of the shaded region in figure 12(c) as the covering space of  $\Pi$ , we see that this has an additional boundary, which is neither  $\mathcal{J}_0$  nor the boundary where a geodesic passes from  $\Pi$  into its complement in  $\mathcal{S}$ . As a result, a geodesic hitting this extra boundary cannot be extended. So, the crucial question is whether the images  $g_2^{-n}(p_1) = g_2^{-n-1}(p_2)$  of the world lines converge inside anti-de Sitter space or not.

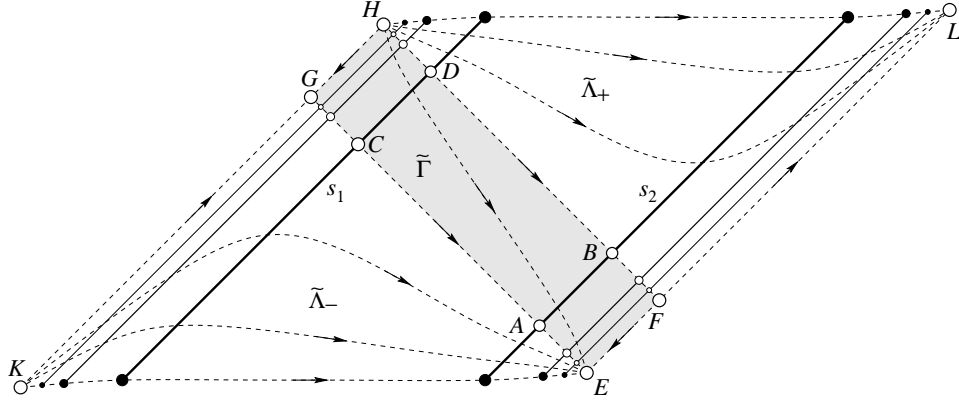


Figure 13: The flow lines of  $\xi_2$  on  $\mathcal{J}_0$  in the region between the two right moving fixed light rays  $KGH$  and  $EFL$ . These are the limits of the images  $g_2^{-n}(s_1) = g_2^{-n-1}(s_2)$  for  $n \rightarrow \pm\infty$ . The total region shown here can be regarded as the covering space of the region in figure 4. What can be seen here as well is that  $G$  is the apparent position of the last point on  $\Lambda_-$  and  $F$  is that of the first point on  $\Lambda_+$ .

Clearly, this depends on whether there are any fixed light rays of  $g_2$ , because the limit would be such a fixed light ray. This is a question that we already answered in the end of section 1. We found that fixed light rays exist if and only if the generating Killing vector of  $g_2$  is of the form (1.12) with  $m$  and  $n$  being two lightlike or spacelike Minkowski vectors of the same length. Now, we know that for the rotational Killing vector  $\xi_{\text{rot}} = \xi_2$  generating  $g_2$ , the Minkowski vectors are given by (A.5), and these are of the same length if and only if  $\mu = \nu$ . Hence, we arrive at the final result that our spacetime is geodesically complete in all cases except for the static one. Indeed, almost all the arguments used above break down in the case  $\delta = 0$ .

### The region of closed timelike curves

Finally, we want to prove some properties of the region  $\Delta \subset \mathcal{S}$ , which is defined to be the union of all closed timelike curves in  $\mathcal{S}$ . The main problem is to show that there is only one such region, or, in other words, that  $\Delta$  is connected. As a by-product, we will also prove some statements about the extremal and the static universes. The actual proof splits into two parts. First we show that a region  $\Delta_0 \subset \Delta$  filled by a special class of closed timelike curves is connected. Then we show that every closed timelike curve passes through  $\Delta_0$ , and therefore  $\Delta$  is also connected.

It is useful to introduce an alternative set of coordinates on the cut surfaces. Let  $(t_-, t_-, \varphi)$ , in spherical coordinates, be a point on the lower face of  $s_1$ , and  $(t_+, t_+, \varphi)$  be its counterpart on

the upper face. We then have the relation (2.7) between  $t_-$  and  $t_+$ , which can be written as

$$\cot t_{\pm} = \tau \pm \beta(\varphi), \quad \beta(\varphi) = \frac{1}{2} \tan \epsilon e^{-\delta} (\cos \varphi + 1) + \frac{1}{2} \tan \epsilon e^{\delta} (\cos \varphi - 1) > 0, \quad (\text{A.11})$$

where  $\tau$  is some real number. Obviously, we can use  $\tau$  and  $\varphi$  as coordinates specifying a physical point on the cut surface  $s_1$  in  $\mathcal{S}$ , and the same coordinates can be introduced on  $s_2$ . Their range is such that  $-\infty < \tau < \infty$  and  $\tanh \delta \leq \cos \varphi < 1$ .

Now, let  $(\tau, \varphi) \in s_1$  and  $(\tau', \varphi') \in s_2$  be two points on the cut surfaces. Can they be connected by a future pointing timelike curve? For this to be the case, the point  $(t'_-, \pi - t'_-, \pi - \varphi')$  on the lower face of  $s_2$  must lie in the future of the point  $(t_+, t_+, \varphi)$  on the upper face of  $s_1$ , with  $t'_-$  and  $t_+$  given by (A.11). To formulate this condition as a function of  $(\tau, \varphi)$  and  $(\tau', \varphi')$ , it is most convenient to use the conformally transformed metric, which of course has the same timelike curves. The question is then whether the spatial distance  $d$  of the two points on the Euclidean sphere, which is given by

$$\cos d = -\cos t_+ \cos t'_- - \sin t_+ \sin t'_- \cos(\varphi + \varphi'), \quad (\text{A.12})$$

is smaller than their time distance  $t'_- - t_+$ , for which we have

$$\cos(t'_- - t_+) = \cos t'_- \cos t_+ + \sin t'_- \sin t_+. \quad (\text{A.13})$$

Comparing the two cosines, we get the condition that

$$-\cot t_+ \cot t'_- > \frac{1}{2}(\cos(\varphi + \varphi') + 1). \quad (\text{A.14})$$

The right hand side is always positive, which implies that the signs of the cotangents must be different. This is only possible if  $t_+ < \pi/2 < t_-$ , because  $t_+$  must be smaller than  $t_-$ . Using (A.11), this can be written as

$$(\beta(\varphi) + \tau)(\beta(\varphi') - \tau') > \frac{1}{2}(\cos(\varphi + \varphi') + 1), \quad (\text{A.15})$$

with the additional condition that both terms in the parenthesis to the left must be positive. This is the condition for a point  $(\tau, \varphi)$  on one of the cut surfaces to be connected to  $(\tau', \varphi')$  on the other cut surface by a future pointing timelike curve.

Now, consider a special class of *symmetric* closed timelike curves, and define  $\Delta_0 \subset \Delta$  to be the union of all these curves. A closed timelike curve is symmetric if it intersects once with each cut surface, at two antipodal points with the same coordinates  $(\tau, \varphi)$ . From (A.15), we get the condition that

$$(\beta(\varphi) + \tau)(\beta(\varphi) - \tau) > \frac{1}{2}(\cos(2\varphi) + 1) \quad \Leftrightarrow \quad \beta^2(\varphi) - \tau^2 > \cos^2 \varphi. \quad (\text{A.16})$$

Whenever this condition is satisfied, then there is a symmetric closed timelike passing through the points with coordinates  $(\tau, \varphi)$  on the two cut surfaces. Take, for example, the grand circles

on the Euclidean sphere, or the true timelike geodesics with respect to the anti-de Sitter metric, connecting the points on the faces of the two cut surfaces.

Before continuing the proof that  $\Delta$  is connected, let us analyze this condition for different values of  $0 < \epsilon < \pi/2$  and  $\delta \geq 0$ . It is easy to show that there is no solution at all for  $e^{-\delta} \tan \epsilon < 1$ . This is also the threshold found in section 3 for the closed lightlike curves on  $\mathcal{J}$  to arise. For  $e^{-\delta} \tan \epsilon > 1$  and  $\delta > 0$ , we find that there is a maximal value of  $\varphi$  for which  $\beta(\varphi) > \cos \varphi$ , namely

$$\cos \varphi > \frac{\tan \epsilon \sinh \delta}{\tan \epsilon \cosh \delta - 1} > \tanh \delta. \quad (\text{A.17})$$

This means that there are symmetric closed timelike curves, but due to the fact that the lower limit of  $\cos \varphi$  is still bigger than  $\tanh \delta$ , they do not reach the world lines of the particles. Remember that on the world lines we have that  $\cos \varphi = \tanh \delta$ . A special situation however arises in the case  $\delta = 0$ . Then, the condition says that  $\cos \varphi$  must be positive, but it can be arbitrarily small. Hence, in the *static* case there are closed timelike curves in every neighbourhood of the point of collision of the particles, which is in the new coordinates on the cut surfaces at  $\tau = 0$  and  $\varphi = \pi/2$ .

In the *extremal* case, where  $e^{-\delta} \tan \epsilon = 1$ , the lower limit for  $\cos \varphi$  becomes 1, which means that the inequality above cannot be satisfied. However, if we include the boundary at  $\varphi = 0$ , then there is exactly one solution where *equality* holds in (A.16), namely  $\varphi = 0$  and  $\tau = 0$ , and this tells us that there is a single closed *lightlike* curve on  $\mathcal{J}$ . Finally, in the *extremal static* case, we have  $\delta = 0$  and  $\epsilon = \pi/4$ , and thus  $\beta(\varphi) = \cos \varphi$ . There is no solution for (A.16), but when equality is allowed we find a series of solutions with  $0 \leq \varphi \leq \pi/2$  and  $\tau = 0$ . This provides a null plane spanned by a family of closed lightlike curves, forming the horizons, as explained in the end of section 4.

Now, let us return to the generic case and the proof that the region of closed timelike curves is connected. It is quite obvious from (A.11) that whenever both  $e^{-\delta} \tan \epsilon$  and  $e^{\delta} \tan \epsilon$  are bigger or equal to one, then  $\beta(\varphi)$  is increasing faster than  $\cos \varphi$  with decreasing  $\varphi$ . In other words, if the condition (A.16) is satisfied for some values of  $\tau$  and  $\varphi$ , then it is also satisfied for the same  $\tau$  and smaller  $\varphi$ . On the other hand, decreasing  $\varphi$  means deforming the symmetric closed timelike curve into the direction of  $\mathcal{J}$ , and for  $\varphi = 0$  it becomes a closed timelike curve on  $\mathcal{J}$ . Hence, every symmetric closed timelike curve can be deformed into a closed timelike curve on  $\mathcal{J}$ .

This proves that the region  $\Delta_0$  filled with symmetric closed timelike curves is connected, because we know that the region  $\Gamma$  of closed timelike curves on  $\mathcal{J}$  is connected. To show that this is also true for the subset  $\Delta \subset \mathcal{S}$  of all closed timelike curves, let  $\lambda$  be such a curve. From section 3 we know that  $\lambda$  intersects alternately with the two cut surfaces. Denote by  $P_n = (\tau_n, \varphi_n)$  the points of intersection, with  $n$  running cyclically around  $\lambda$ . Since each part of  $\lambda$  between  $P_n$  and  $P_{n+1}$  must be a timelike curve, we get the condition that, for all  $n$ ,

$$(\beta(\varphi_n) + \tau_n)(\beta(\varphi_{n+1}) - \tau_{n+1}) > \frac{1}{2}(\cos(\varphi_n + \varphi_{n+1}) + 1) > \cos \varphi_n \cos \varphi_{n+1}. \quad (\text{A.18})$$

The right hand side of these inequalities are all positive, because  $\varphi_n < \pi/2$ , and therefore we can multiply them. This yields

$$\prod_n (\beta^2(\varphi_n) - \tau_n^2) > \prod_n \cos^2 \varphi_n. \quad (\text{A.19})$$

The factors to the left are also positive, which implies that at least for one of them we have

$$\beta^2(\varphi_n) - \tau_n^2 > \cos^2 \varphi_n. \quad (\text{A.20})$$

But this is exactly the condition (A.16) for a symmetric closed timelike curve, which means that the point  $P_n$  on  $\lambda$  lies in the subset  $\Delta_0$  of symmetric closed timelike curves. This completes the proof that  $\Delta$  is connected.

## References

- [1] Gott J R 1991 Closed timelike curves produced by pairs of moving cosmic strings *Phys.Rev.Lett.* **66** 1126
- [2] Bañados M, Teitelboim C and Zanelli J 1992 The black hole in three-dimensional space-time *Phys. Rev. Lett.* **69** 1849
- [3] Bañados M, Henneaux M, Teitelboim C and Zanelli J 1993 Geometry of the (2+1) black hole *Phys. Rev. D* **48** 1506
- [4] Ellis G F R and Hawking S W 1973 *The large scale structure of space-time* (Cambridge University Press)
- [5] Grant J D E 1993 Cosmic strings and chronology protection *Phys. Rev. D* **47** 2388
- [6] Matschull H-J 1999 Black hole creation in 2+1 dimensions *Class. Quantum Grav.* **16** 1069
- [7] Mann and Ross 1993 Gravitationally collapsing dust in (2+1)-dimensions *Phys. Rev. D* **47** 3319
- [8] Deser S, Jackiw R and 't Hooft G 1984 Three dimensional Einstein gravity: dynamics of flat space *Ann.Phys.* **152** 220
- [9] Matschull H-J and Welling M 1998 Quantum mechanics of a point particle in (2+1)-dimensional gravity *Class. Quantum Grav.* **15** 2981
- [10] Deser S and Steif A R 1992 Gravity theories with lightlike sources in  $D = 3$  *Class. Quantum Grav.* **9** L153
- [11] Cutler C 1992 Global structure of Gott's two-string space-time *Phys.Rev. D* **45** 487

- [12] Abramowicz M A, Carter B, Lasota J P 1988 Optical reference geometry for stationary and static dynamics *Gen. Rel. Grav.* **20** 1173
- [13] Balasz N L and Voros A 1986 Chaos on the pseudosphere *Phys. Rep.* **143** 109
- [14] Åminneborg S, Bengtsson I and Holst S 1999 A spinning anti-de Sitter wormhole *Class. Quantum Grav.* **16** 363
- [15] Åminneborg S, Bengtsson I, Brill D R, Holst S and Peldán P 1998 Black holes and wormholes in (2+1)-dimensions *Class. Quantum Grav.* **15** 627
- [16] Deser S, Jackiw R 1984 Three dimensional cosmological gravity: dynamics of constant curvature *Ann. Phys.* **153** 405
- [17] Penrose R 1972 The geometry of impulsive gravitational waves, in *General Relativity, Papers in honour of J L Synge* O’Raifeartaigh (ed) (Oxford University Press)
- [18] Aichelburg and Sexl 1971 On the gravitational field of a massless particle *Gen. Rel. Grav.* **2** 303
- [19] Deser S and Steif A R 1993 No time machines from lightlike sources in 2+1 gravity, in *Directions in General Relativity: Proceedings of the 1993 International Symposium, Maryland* vol. 1 Hu B L, Ryan M P and Vishveshwara C V (eds) (Cambridge University Press)
- [20] Thorne K S 1993 in *General Relativity and Gravitation 1992, Proceedings of GR13 held at Cordoba, Argentina* Gleiser R J, Kozameh C N, Moreschi O M (eds) (IOP Publishing Ltd)
- [21] Wald R M 1994 *Quantum Field Theory in Curved Spacetime and Black Hole Thermodynamics* (The University of Chicago Press)